이학박사학위논문

RNA 가수분해효소 SAMHD1 의 HIV-1 억제 기능에 대한 연구

Role of ribonuclease SAMHD1 in HIV-1 restriction

2015 년 2 월

서울대학교 대학원

협동과정 유전공학전공

유 정 민

CONTENTS

MATERIALS AND METHODS

RESULTS

LIST OF TABLES AND FIGURES

LIST OF ABBREVIATIONS

SAMHD1 : sterile alpha motif (SAM) domain and HD domain-containing protein 1

HIV : human immunodeficiency virus

RT : reverse transcriptase

DC :dendritic cell

IFN : interferon

ISG : interferon-stimulated gene

dNTPase : deoxynucleotide triphosphohydrolase

dGTP : deoxyguanosine triphosphate

CDK1 : cyclin-dependent kinase 1

AGS : Aicardi-Goutières syndrome

SLE : systemic lupus erythematosus

ssDNA : single-stranded DNA

dsDNA : double-stranded DNA

ssRNA : single-stranded RNA

dsRNA : double-stranded RNA

RNASEH2 : ribonuclease H2

ADAR1 : adenosine deaminase acting on RNA 1

PMA :phorbol-12-myristate-13-acetate

RIP : RNA immunoprecipitation

MDM : monocyte-derived macrophage

qRT-PCR : quantitative reverse transcription-PCR

h.p.i : hour post-infection

ABSTRACT

Role of ribonuclease SAMHD1 in HIV-1 restriction

Jeongmin Ryoo
Department of Interdisciplinary Program
in Genetic Engineering
The Graduate School
Seoul National University

Sterile alpha motif (SAM) domain and HD domain-containing protein 1 (SAMHD1) is a host cell restriction factor that inhibits HIV-1 replication by impairing reverse transcription in non-cycling cells such as macrophages, dendritic cells and resting $CD4^+$ T cells. SAMHD1 has a dGTP-induced dNTPase activity, and therefore was initially proposed to deplete intracellular dNTP level below the levels required for reverse transcription of HIV-1. However, the phosphorylation of SAMHD1 at position T592 regulates its ability to restrict HIV-1 without decreasing cellular dNTP levels, which is not consistent with a role for SAMHD1 dNTPase activity in HIV-1 restriction. Here, I show that SAMHD1 possesses RNase activity and that the RNase but not the dNTPase function is essential for HIV-1 restriction. By enzymatically

characterizing Aicardi-Goutières syndrome (AGS)-associated SAMHD1 mutations and mutations in the allosteric dGTP-binding site of SAMHD1 for defects in RNase or dNTPase activity, I identify SAMHD1 point mutants that cause loss of one or both functions. The RNase-positive and dNTPase-negative $SAMHD1_{D137N}$ mutant is able to restrict HIV-1 infection, whereas the RNase-negative and dNTPase-positive $SAMHD1_{Q548A}$ mutant is defective for HIV-1 restriction. SAMHD1 associates with HIV-1 RNA and degrades it during the early phases of cell infection. SAMHD1 silencing in macrophages and $CD4^+$ T cells from healthy donors increases HIV-1 RNA stability, rendering the cells permissive for HIV-1 infection. Furthermore, the phosphorylation of SAMHD1 at T592 negatively regulates its RNase activity in cells and consequently the ability of SAMHD1 to restrict HIV-1 infection. My results reveal that the RNase activity of SAMHD1 is responsible for preventing HIV-1 infection by directly binding and degrading the HIV-1 RNA.

Keywords: HIV-1, SAMHD1, RNase

Student number: 2008-20250

INTRODUCTION

Human immunodeficiency virus (HIV) — HIV-1 and HIV-2 — causes AIDS and belong to a group of retroviruses that are endemic to African apes and Old World monkeys and are known as the primate lentiviruses. HIV-1, which is responsible for the global AIDS pandemic, and HIV-2, which causes AIDS in regions of West Africa, are mainly spread by heterosexual transmission and replicate in $CD4^+$ T cells and macrophages. HIV infection results in the depletion of $CD4^+$ T cells, immunodeficiency and the eventual onset of life-threatening opportunistic infections.

HIV enters T cells and macrophages via binding of the viral envelope protein gp120 to the coreceptor CD4. The envelope subunit gp41 interacts the coreceptor CCR5 or CXCR4 on the target-cell membrane, inducing fusion of the viral envelope with the plasma membrane. Once the viral core is released into the cytosol, HIV reverse transcriptase (RT) converts RNA into DNA in the reverse-transcription complex. That complex matures into the preintegration complex, which delivers reverse-transcribed HIV DNA to the nucleus for chromosomal integration (Figure 1). Few copies of HIV DNA integrate; thus, the bulk of HIV DNA is left behind in the cytosol to be cleared by host enzymes. Once the viral genomic DNA is integrated into a host chromosome, viral transcription is activated by host pathways with the assistance of the HIV

protein Tat. HIV mRNAs are all capped and polyadenylated. The unspliced RNA is both translated to generate the Gag and Pol proteins and incorporated as genomic RNA into nascent virions at cell-membrane sites where the envelope and capsid proteins assemble before budding.

Mucosal innate immunity is the first line of defense against HIV-1 during the early phase of infection, and it also has a crucial role in shaping ensuing adaptive immune responses. There are two major types of innate immunity involved in HIV-1 infection: cellular and intracellular. Cellular innate immunity includes functions of dendritic cells (DCs) that are among the first group of cells that contact HIV-1 at the site of infection and that can mediate the trans-infection of $CD4^+$ T cells (1). The $\gamma\delta^+$ T cells play key role in innate responses to HIV by generating antiviral factors such as RANTES, MIP-1α and MIP-1β (2). Natural killer (NK) cells also serve cellular innate immunity to HIV by eliminating infected cells and regulating DC functions (3). Intracellular innate immunity includes intrinsic immunity mediated by host factors with important roles in restricting HIV-1 replication, such as TRIM5α, APOBEC3G, tetherin Figure 1). All of these restriction factors are also encoded by interferon (IFN)-stimulated genes (ISGs). HIV-1 has evolved effective ways to evade some of these restriction factors via accessory proteins, such as Vif to counteract APOBEC3G and Vpu to degrade tetherin (4-6). Recent studies reported that

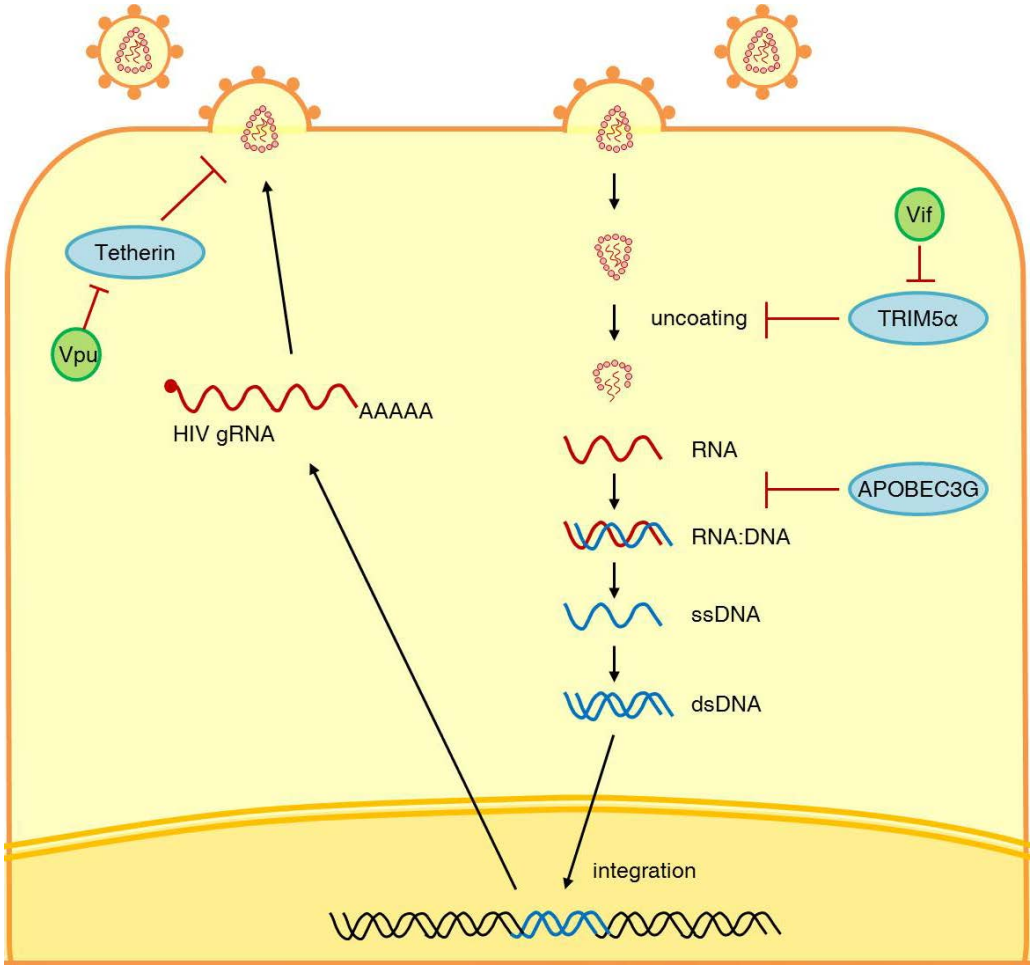
Tetherin
Vpu
HIV gRNA
AAAAA
Vif
uncoating
TRIM5α
RNA
APOBEC3G
RNA:DNA
ssDNA
dsDNA
integration

Figure 1. Schematic overview of HIV-1 life cycle and restriction factors of HIV-1.

The classical entry route of HIV-1 in target cells is through attachment at the cell surface and fusion. The viral core is delivered in the cytoplasm. After or concomitantly with uncoating and nuclear import steps, reverse transcription occurs. When reverse transcription and nuclear import are completed, the viral genome is integrated into the host's genome. The provirus is transcribed, exported and translated to give rise to the viral proteins that assemble at the plasma membrane, to give rise to new virions that can bud from the cell. Many steps of the HIV-1 life cycle are targeted by antiviral factors such as TRIM5α, APOBEC3G, tetherin. HIV-1 has evolved strategies to counteract these intrinsic antiviral factors, through accessory proteins such as Vif, Vpu.

SAMHD1 is a novel HIV-1 restriction factor in non-cycling myeloid cells and resting $CD4^+$ T cells (4-6). In addition to HIV-1, SAMHD1 also blocks diverse retroviruses (7, 8). However, the mechanisms of SAMHD1-mediated retrovirus restriction and its physiological functions remain to be elucidated.

1. Identification of SAMHD1 as an HIV-1 restriction factor

Several studies have shown that while wild-type HIV-2 viruses grow well in human monocyte-derived DCs, growth of these Vpx-deletion mutants is completely suppressed, demonstrating that Vpx encoded by SIV and HIV-2 is essential for viral replication in cells of myeloid lineage (9, 10). Vpx is critical for HIV-2 infection in human macrophages by enhancing the efficiency of viral reverse transcription (10, 11). Further studies indicated that Vpx recruits a Cul4-DDB1-DCAF1 E3 ubiquitin ligase complex and induces proteasome-degradation of an unknown restriction factor (11, 12). SAMHD1 was identified as a Vpx-interacting protein by mass spectrometry and turned out to be this putative HIV-1 restriction factor (4, 5). Knockdown of endogenous SAMHD1 in differentiated human monocytic THP-1 cells leads to accumulation of full-length HIV DNA. Conversely, overexpression of SAMHD1 in U937 cells inhibits HIV-1 infection by blocking early reverse transcription step.

1.1 Structure and enzymatic activities of SAMHD1

SAMHD1 is highly expressed in myeloid cells (4, 5) and was initially identified as the human ortholog of the mouse gene *Mg11*, which is induced by IFNγ treatment of macrophages and DCs (13). SAMHD1 expression is also induced in human macrophages following IFN-stimulatory DNA treatment in an IFN-dependent fashion (14, 15). SAMHD1 protein consists of two domains; sterile alpha motif (SAM) domain and HD domain (Figure 2). SAM domains are protein-protein interaction motif and can also bind RNA (16). HD domains are characterized by a motif of doublet cation-coordinating His and Asp residues (H. . .HD. . .D) (17). The HD domains in proteins have putative nucleotidase and phosphodiesterase activities. Actually, it has been demonstrated that SAMHD1 is a dGTP-activated deoxynucleotide triphosphohydrolase (dNTPase) which cleaves deoxynucleoside triphosphates (dNTP) into their deoxynucleosides (dN) and inorganic triphosphates (18). dGTP-induced SAMHD1 tetramerization is required for dNTPase activity (19, 20). In addition to its triphosphohydrolase activity, SAMHD1 also has a metal-dependent 3'-5' exonuclease activity that degrades single-stranded RNA (ssRNA) or single-stranded DNA (ssDNA) (21). Both enzymatic activities require the same active sites. These catalytic active sites are responsible for HIV-1 restricion.

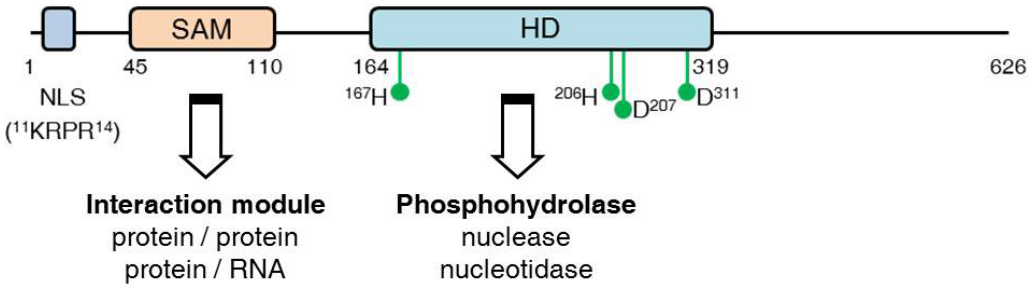

Figure 2. Schematic illustration of SAMHD1 protein.

SAMHD1 is a 626-amino acid protein that contatins an SAM and HD domain. NLS is located in N-terminus of SAMHD1.

SAMHD1 is a predominantly nuclear protein and the nuclear localization signal (NLS) of SAMHD1 protein has been identified to residues ^{11}KRPR^{14} in the N-terminus of the protein (22, 23). But SAMHD1 is also found in the cytoplasm (6). Mutations in NLS of SAMHD1 changed its nuclear distribution to the cytoplasm. Cytosolic SAMHD1 can still restrict HIV-1 similar to the wild-type protein.

2. Mechanisms of SAMHD1-mediated retroviral restriction

2.1 Inhibition retroviral reverse transcription by depleting intracellular dNTP pool.

It was demonstrated that intracellular nucleotide levels can regulate retroviral infection efficiencies in cells (24). It has been also known that low levels of deoxynucleotides in peripheral blood lymphocytes could be a means to inhibit HIV-1 replication (25). Efficient HIV-1 infection in macrophages depends on the efficient cellular dNTP utilization by RT (26). Due to low cellular dNTP content in resting cells and non-cycling cells, HIV-1 entry into quiescent primary lymphocytes can initiate reverse transcription but cannot complete the full-length HIV-1 cDNA synthesis (27). Recently, SAMHD1 was demonstrated to restrict HIV-1 replication by hydrolyzing dNTPs to deoxynucleosides and

inorganic triphosphate in a deoxyguanosine triphosphate (dGTP)-dependent fashion. SAMHD1 reduces cellular dNTP concentrations below the levels required for retroviral reverse transcription (4, 5, 18, 28-30) (Figure 3). SAMHD1-mediated HIV-1 restriction in resting $CD4^+$ T cells is also dependent on low dNTP levels in the cells (6). Furthermore, it was demonstrated that SAMHD1 restricts HIV-1 infection in monocyte-derived DCs by dNTP depletion since Vpx-mediated SAMHD1 degradation significantly increased intracellular dNTP concentrations (31). These studies indicate a strong correlation between low levels of cellular dNTPs and inhibition of HIV-1 replication. However, addition of dN into resting $CD4^+$ T cells or macrophages to increase the intracellular dNTP pool cannot fully restore HIV-1 or SIV infections (6, 30), suggesting that decreasing dNTP pool by SAMHD1 may not be the sole mechanism underlying retroviral restriction in non-dividing cells.

2.2 Phosphorylation of SAMHD1 negatively regulates its HIV-1 restriction ability.

Two previous studies reported that phosphorylation of SAMHD1 at Thr 592 impairs its HIV-1 restriction function (32, 33). However, mutagenesis studies indicated that T529 phosphorylation of SAMHD1 does not affect its dNTPase activity (32). SAMHD1 has a target motif for cyclin-dependent kinase 1 (CDK1)

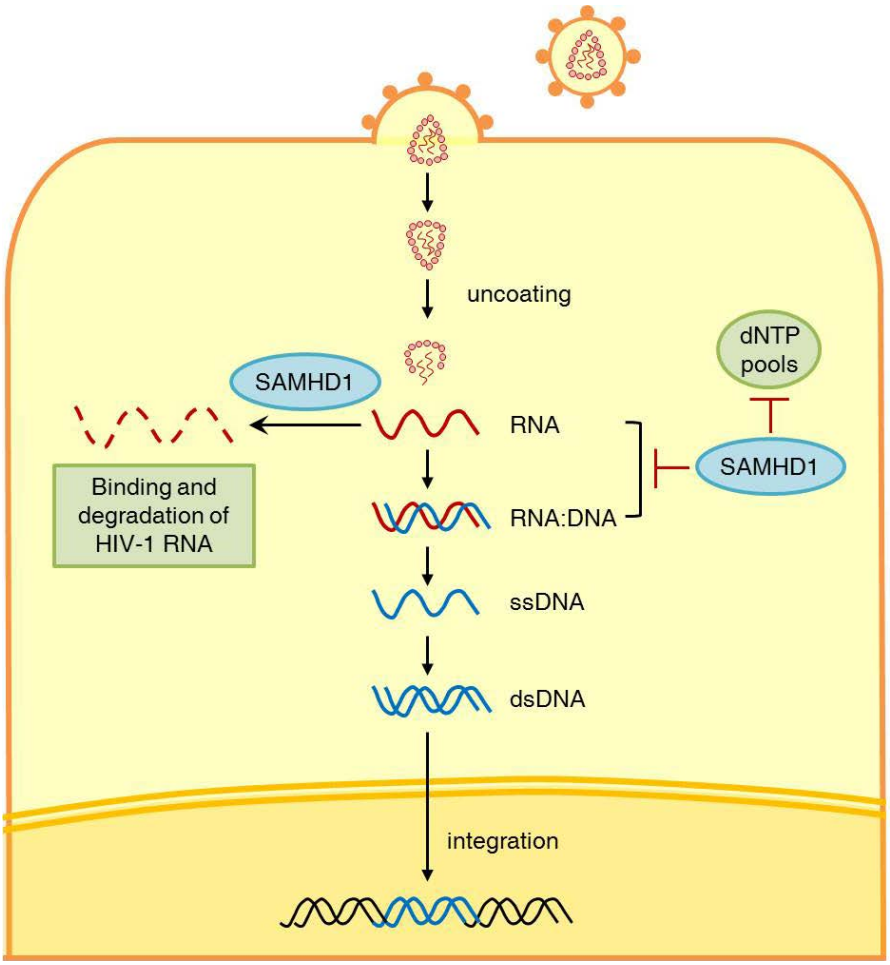

Figure 3. Proposed mechanisms of SAMHD1-mediated HIV-1 restriction.

SAMHD1 possesses two enzymatic activities. SAMHD1 functions as a dNTPase to decrease intracellular dNTP pool and thereby limits HIV-1 DNA synthesis during reverse transcription. Furthermore, SAMHD1 may directly bind and degrade HIV-1 genomic RNA in the infected cell.

and CDK1 is necessary for SAMHD1 phosphorylation. SAMHD1 phosphorylation regulates ability of HIV-1 restriction, but not the cellular levels of dNTPs. Thus, SAMHD1-mediated HIV-1 inhibition may be independent of its dNTPase activity, suggesting additional cellular mechanisms may contribute to SAMHD1-mediated HIV-1 restriction function (Figure 4). One possibility is that phosphorylation of SAMHD1 may alter its structure or conformation and thereby regulate its HIV-1 restriction function. A second possibility is that phosphorylation of residue T592 controls the ability of SAMHD1 to interact with an unknown cofactor required for retroviral restriction.

2.3 SAMHD1-mediated HIV-1 inhibition may involve its nuclease activity.

In addition to the dNTPase activity of SAMHD1, recent studies suggest that SAMHD1 can bind to and degrade HIV-1 RNA, which can be a novel mechanism blocking retroviral infection (21, 34, 35). SAMHD1 was identified as a nucleic-acid-binding protein displaying a preference for RNA over DNA (34). It was demonstrated that ssRNA and ssDNA can promote the formation of the SAMHD1 complex (35). SAMHD1 associates with endogenous nucleic acids *in situ*. Using fluorescence cross-correlation spectroscopy, it was also shown that SAMHD1 specifically interacts with ssRNA and ssDNA. The formation of SAMHD1 complexes appears to be nucleic-acid-binding dependent. The

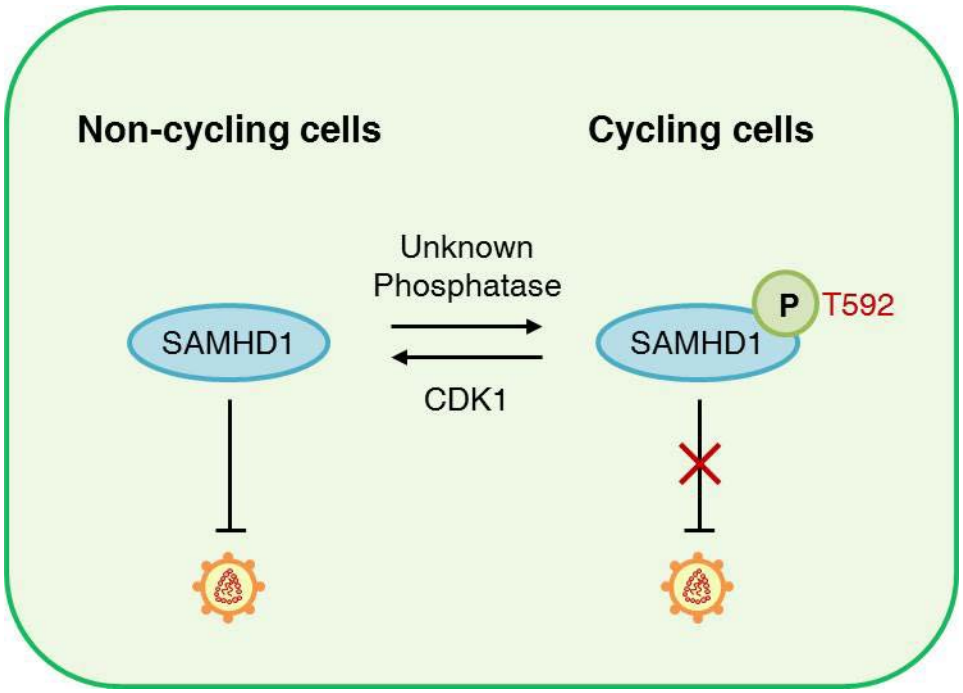

Figure 4. Model for the regulation of SAMHD1 restriction activity by phosphorylation at the T592.

SAMHD1 only exhibits antiretroviral activity when expressed in non-cycling cells because SAMHD1 is unphosphorylated in non-cycling cells. Phosphorylated at T529 of SAMHD1 is repressive for HIV-1 restriction in cycling cells.

interaction with nucleic acids and complex formation requires the HD domain and the C-terminal region of SAMHD1, but not the SAM domain. Furthermore, mutations associated with AGS exhibit both impaired nucleic acid-binding and complex formation implicating that interaction with nucleic acids is an important function of SAMHD1 (35). These results highlight an important role of SAMHD1 in nucleic acid metabolism. Notably, Beloglazova et al. have reported exonuclease activity of recombinant SAMHD1 protein (21). They found that purified full-length human SAMHD1 protein from *E. coli* possesses metal-dependent 3'-5' exonuclease activity degrading ssRNA and ssDNA *in vitro*. SAMHD1 also exhibits strong binding to DNA and RNA with complex secondary structures.

Together, these observations that there are the interactions between nucleic acids and SAMHD1 and SAMHD1 has exonuclease activity suggest that SAMHD1 may directly bind to and degrade retroviral genomic RNA in the infected cells (Figure 3). However, this hypothesis remains to be elucidated in HIV-1 infected cells. Further clarification of the mechanisms underlying SAMHD1-mediated HIV-1 RNA binding and degradation is important for fully understanding the HIV-1 restriction in non-cycling cells.

3. SAMHD1 and Aicardi-Goutières syndrome

Mutations in SAMHD1 gene are associated with Aicardi-Goutières syndrome (AGS) (14). AGS is a genetic autoimmune disorder that mimics congenital viral infection and is characterized by the aberrant production of type I interferon (IFN) (36). A disturbance of IFNα homeostasis is central to the pathogenesis of the prototypic autoimmune disorder systemic lupus erythematosus (SLE) (37-39). In keeping with this, AGS clinically overlaps with SLE and some children with AGS develop an early-onset form of SLE (40-43). AGS can be caused by mutations in any of genes encoding TREX1 (*AGS1*) (44), 3′-5′ exonuclease with substrate preference for single-stranded DNA (ssDNA); the three components of the ribonuclease H2 (RNASEH2) endonuclease complex (*AGS2, 3 and 4*) (45), which cleaves the RNA moiety of RNA:DNA hybrids (46); adenosine deaminase acting on RNA 1 (ADAR1) (*AGS6*) (47), an RNA editing enzyme; MDA5 (*AGS7*, also known as IFIH1) (48), an innate sensor of viral RNA (49) (Figure 5).

Trex1$^{-/-}$ mice spontaneously develop autoimmune multiorgan inflammation, which can be rescued by inactivation of the type I IFN system, demonstrating the critical pathogenic role of the IFN response (50-52). These findings led to a new concept of autoimmunity caused by defects of nucleic acid metabolism

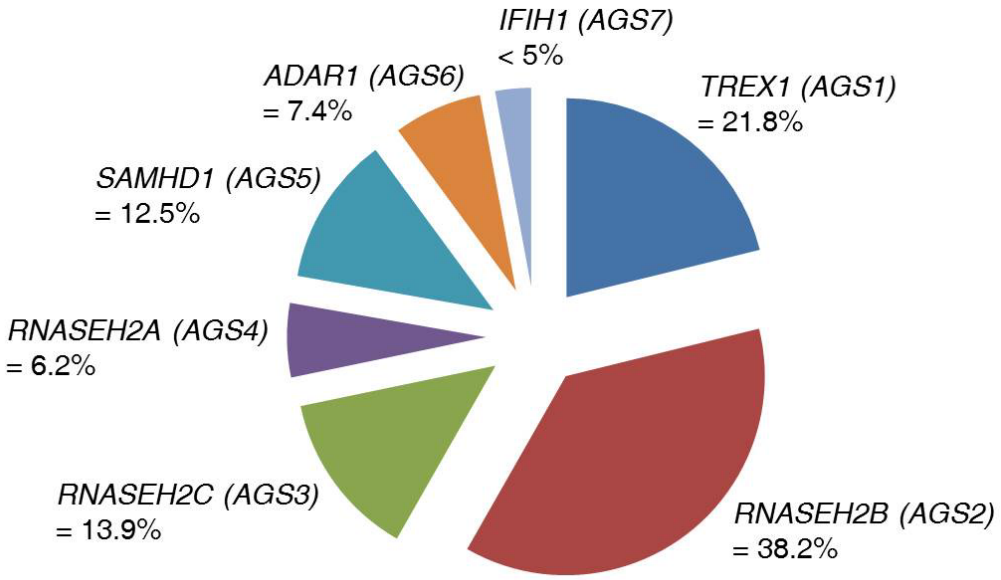

Figure 5. Genes identified to be associated with the AGS.

Percentages of families with AGS with either biallelic or recognized dominant mutations in *TREX1*, *RNASEH2A*, *RNASEH2B*, *RNASEH2C*, *SAMHD1*, *ADAR1*, or *IFIH1*.

resulting in intracellular accumulation of endogenous nucleic acids, which in turn trigger a type I IFN response (51) (Figure 6). Short ssDNA species derived from during DNA replication intermediates (53) or intermediates of endogenous retroelements (51) were proposed to be responsible for activation of the IFN system in *Trex1*$^{-/-}$ mice. Trex1 can also metabolize HIV reverse transcripts within infected cells (54), suggesting a key role in anti-retroviral defense and in clearance of nucleic acids derived from endogenous retroelements to avoid autoimmune disease.

Loss of ADAR1 in mice is embryonically lethal and *Adar1*$^{-/-}$ mouse embryos, like *Trex1*$^{-/-}$ mice, display spontaneous production of type I IFN (55). ADAR1 catalyze the deamination of adenosine to inosine. Recently, A-to-I RNA editing inhibits antiviral inflammatory and IFN responses by altering RNA-sensing innate immune signaling. Mice deficient for RNase H2 accumulate ribonucleotides in genomic DNA, resulting in a spontaneous DNA damage response (56, 57).

Two recent studies reported the generation of *samhd1*-knockout mouse models (58, 59). Unlike the severe autoimmune disease in SAMHD1-deficient human patients with AGS, the *samhd1*-null mice were healthy beyond the age of 96 weeks. Spontaneous IFN production and significant induction of ISGs were observed in *samhd1*-null mice. However, *Samhd1*$^{-/-}$ mice did not display

detectable amounts of circulating IFN proteins or upregulation of ISG products in their sera. These observations suggest that SAMHD1 deficiency in mice is not sufficient to enhance the production or release of type I IFNs and mouse SAMHD1 function might be redundant or not directly involved in the innate immune responses to nucleic acids in mice. Further studies are needed to explore mechanisms behind AGS pathogenesis in deficiency of SAMHD1.

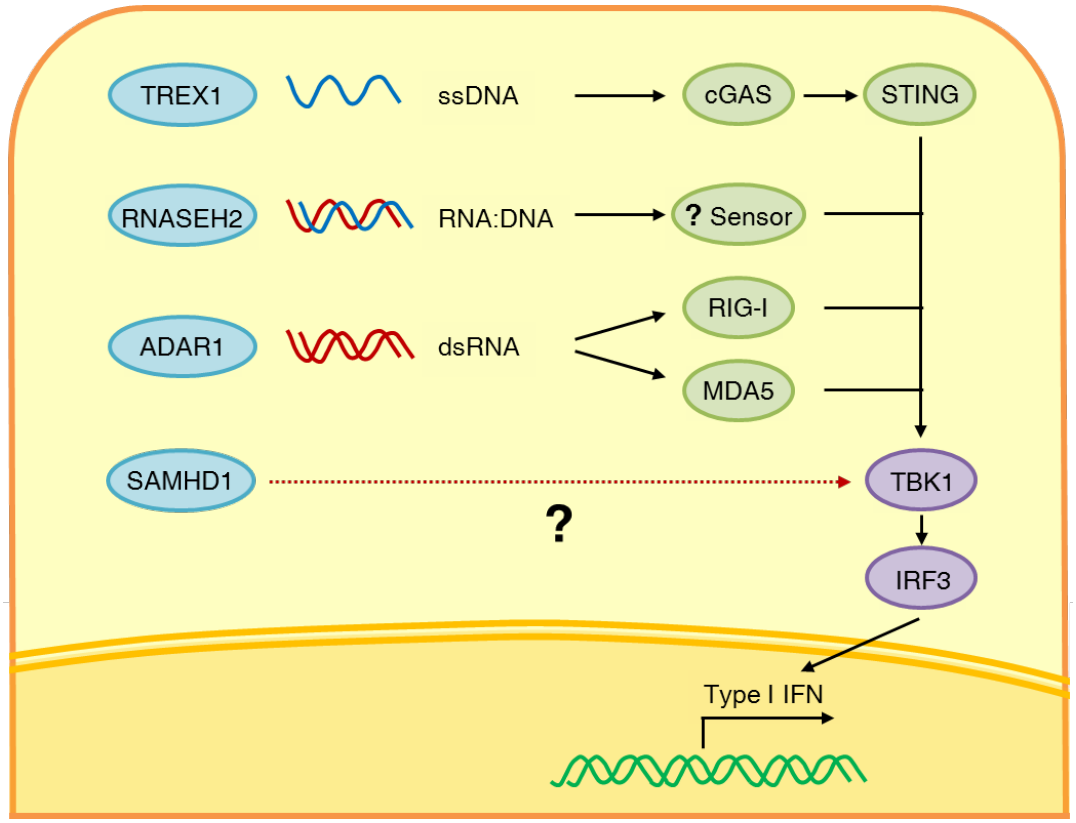
TREX1
ssDNA
cGAS
STING
RNASEH2
RNA:DNA
? Sensor
ADAR1
dsRNA
RIG-I
MDA5
SAMHD1
?
TBK1
IRF3
Type I IFN

Figure 6. Model of AGS pathogenesis.

Lack of TREX1 activity results in accumulation of ssDNA thereby augmenting the pool of nucleic acids in the cytoplasm. ssDNA is recognized by cGMP-AMP synthase (cGAS), DNA sensor. Unmodified self-RNAs due to lack of function mutations are sensed by RIG-I and MDA5. RNASEH2 and SAMHD1 would also impair the control of nucleic acid homeostasis and activate type I IFN pathway through unknown sensors.

MATERIALS AND METHODS

1. Ethics statement

Adult blood samples were anonymously provided by the Blood Center of the Korean Red Cross, Seoul, under the approval of the Institutional Review Board of Korean Red Cross with consent for research use. Written informed consent was obtained from the blood donors with the approval of the Ethics Committee of the Korean Red Cross. Experiments involving human blood were approved by the Institutional Review Board at Seoul National University (SNUIRB No. E1304/001-023).

2. Plasmids

Full-length human SAMHD1 was amplified by PCR from cDNA generated by the reverse transcription of RNA from HeLa cells, and the PCR product was inserted into a pGEX-4T-1 vector and a pMSCV-puro vector. The $SAMHD1_{D207N}$, $SAMHD1_{D311A}$, $SAMHD1_{D137N}$ and $SAMHD1_{Q548A}$ mutants were generated using the nPfu-forte DNA Polymerase Kit (Enzynomics). Retroviral vectors encoding the wild-type or T592 phosphorylation variants SAMHD1 were described previously8. HIV-1-GFP, pLaiΔenvGFP3, and HCMV-VSV-G were described previously (60).

3. Protein expression and purification

The GST-tagged, full-length, human SAMHD1 proteins (GST-SAMHD1) were expressed in E. coli Rosetta (λDE3) (Novagen). The Rosetta cells were grown in Terrific broth containing ampicillin (100 μg/ml) at 37 °C to an optical density (OD) 600 of 2.0, and the cells were rapidly cooled on ice to 16 °C. After induction with 0.1 mM isopropyl-β-D-thiogalactopyranoside (IPTG; Ducheba), the cells were allowed to grow for 16 h at 16 °C. The E. coli pellet containing the GST fusion protein was lysed with PBS, and the protein was purified using glutathione-Sepharose column chromatography, as previously described (61).

4. Preparation of DNA and RNA substrates

Fragments of the HIV-1 5' LTR, gag, and 3' LTR were transcribed in vitro using T7 RNA polymerase (Enzynomics). The transcripts were purified using denaturing polyacrylamide gel electrophoresis (PAGE; 5% polyacrylamide/8 M urea). Synthetic DNA and RNA oligonucleotides were 5'-end labeled with ^{32}P using T4 polynucleotide kinase and [γ-^{32}P]ATP. The nucleotides were precipitated by the addition of 3 M ammonium acetate and 100% (vol/vol) ethanol. The nucleotides pellets were washed with 75% ethanol, dried and resuspended in 10 mM Tris-Cl (pH 7.8) containing 1 mM EDTA. The synthetic

dsDNAs and dsRNAs (Table 1) were prepared by annealing the oligonucleotides.

5. *In vitro* nuclease assay

Assays were performed in 20-μl reaction mixtures containing PBS supplemented with 5 mM $MgCl_2$, 2 mM DTT, 10% glycerol, 0.01% NP-40, ^{32}P-labeled nucleic acid substrates, and purified recombinant proteins (150 nM) or immunoprecipitated proteins at 37 °C for the indicated times. The reactions were stopped by the addition of an equal volume of formamide loading buffer and then boiled. The products were separated in 15% polyacrylamide gels containing 8 M urea and buffered with 0.5 × Tris-borate-EDTA (TBE) and then analyzed by autoradiography using a phosphorimager (BAS2500, Fujifilm).

6. dGTP-triphosphohydrolase assay

An enzymatic assay based on thin layer chromatography was performed as described previously (28). The purified recombinant protein was incubated in 50 mM Tris-HCl (pH 8.0), 20 mM KCl, 5 mM $MgCl_2$, 0.1 μCi [α-^{32}P]dGTP, and 200 μM cold dGTP for 3 h at 37 °C. The reactions were stopped by heat-inactivation at 70 °C for 10 min. The reaction mixtures were spotted along with

dGMP, dGDP, and dGTP standards onto polyethyleneimine (PEI)-cellulose plates (Sigma-Aldrich) and subsequently separated using a mobile phase of 1.2 M LiCl. After separation, the α-^{32}P-labeled reaction products were visualized using a phosphorimager, and the migration indicators were detected by UV-C (254 nm).

7. Cells and reagents

U937 and THP-1 cells were cultured in RPMI 1640 supplemented with 10% fetal bovine serum (Hyclone), 2 mM GlutaMAX-I, 100 U/ml penicillin, and 100 μg/ml streptomycin (Invitrogen). HEK293T cells and Phoenix Ampho cells were cultured in DMEM supplemented as described for RPMI 1640. Stable U937 cells expressing SAMHD1 proteins were obtained by retroviral infection. The pMSCV-puro construct was used to transfect Phoenix Ampho cells using the calcium phosphate method. Two days later, the retrovirus-containing supernatant was used to transduce U937 cells by spin infection with 8 μg/ml polybrene. The transduced cells were selected in 1 μg/ml puromycin. Peripheral blood mononuclear cells (PBMCs) were obtained from human blood by density gradient centrifugation using Ficoll-Paque Plus™ (Amersham Healthcare). Monocytes were isolated from the PBMCs using a magnetic bead-

based positive selection kit (IMagTM) and anti-human CD14 beads (BD Biosciences). This procedure routinely yielded over 90% pure $CD14^+$ cells, as verified by flow cytometry. Monocyte-derived macrophages (MDMs) were obtained from monocytes by culturing the cells for 3 days with GM-CSF (10 ng/ml) and M-CSF (20 ng/ml). $CD4^+$ T cells were isolated from the PBMCs using a magnetic bead-based positive selection kit (IMagTM) and anti-human CD4 beads (BD Biosciences). T cells were activated, and post-activation resting T cells were obtained as previously described (6). Resting $CD4^+$ T cells (2×10^6 cells/ml) were treated overnight with PHA-L (2 mg/ml). The next day, the medium was exchanged and cells were incubated in RPMI medium with 20 IU/ml IL-2 for 3 days. Activated $CD4^+$ T cells were electroporated with SAMHD1-specific siRNA or non-specific siRNAs. The siRNA-treated cells were cultivated in RPMI medium with gradually reducing concentrations of IL-2. The activation state of CD4+ T cells was analyzed by monitoring the surface expression of the activation markers CD25 and CD69. The experimental design for the time course analysis of MDMs and $CD4^+$ T cells is shown in Figure 27A and 28A.

8. RNA interference

siRNA targeting SAMHD1 was purchased from Dharmacon. MDMs and $CD4^+$ T cells (2×10^6 cells) were electroporated in 100-µL reactions with siRNA (10 nM) using the Neon Transfection System (Invitrogen). Transfections with ON-TARGETplus Non-targeting pool (Dharmacon) were performed in parallel as a negative control. The MDMs and $CD4^+$ T cells were pulsed once each for 20 ms at 2150 and 2100 volts, respectively.

9. Viruses and VLP production

HEK293T cells were transfected with 10 µg of HIV-1-GFP, HIV-1_{D443N}-GFP or pLaiΔenvGFP3 and 2 µg of HCMV-VSV-G using the calcium phosphate method. Vpx-containing and control VLPs were generated by the transfection of HEK293T cells with pSIV3+ or pSIV3+ Δvpx. Culture supernatants were collected and filtered (0.45 µm) 48 h after transfection. U937 cells (0.5×10^6 cells/ml) were seeded in 12-well plates and differentiated for 20 h in PMA (phorbol-12-myristate-13-acetate, 30 ng/ml). The cells were infected with 100 ng of pseudotyped viruses for 2 h. The cells were then washed and cultured for 48 h. Infected cells were analyzed by flow cytometry or qRT-PCR.

10. Quantitative real-time PCR

VSV-G-pseudotyped HIV-1-GFP-infected cells were harvested at various time points, and DNA was isolated using the QIAamp Blood DNA Minikit (Qiagen). qPCR was performed with the iCycler iQ real-time PCR detection system (BioRad) using HIV-1-specific primers: R/U5 (forward, GCCTCAATAAA GCTTGCCTTGA; reverse, TGACTAAAAGGGTCTGAGGGATCT) and U5/ψ (forward, TGTGTGCCCGTCTGTTGTGT; reverse, GAGTCCTGCGTCGAGAG ATC). RNA isolation from HIV-1-GFP-infected cells or SAMHD1-silenced THP-1 cells was performed at various time points according to the manufacturer's instructions (Invitrogen). One microgram of RNA was treated with DNase I prior to qPCR analysis and isolated by phenol:chloroform extraction. The data were normalized to an internal control gene, MDM2 or β-actin. The purified RNA was reverse transcribed using random primers, and real-time PCR was performed with the iCycler iQ real-time PCR detection system (BioRad) using HIV-1-specific primers (Table 2).

Table 1. Synthetic nucleic acids used in nuclease assays.

Oligomer	Sequence
20-bp ssRNA	5'-CUCCAUCACCCUCCAUCACC-3'
30-bp ssRNA	5'-ACCCACUGAAUCAGAUAAAGAGUUGUGUCA-3'
20-bp dsRNA	5'-CUCCAUCACCCUCCAUCACC-3'
	3'-GAGGUAGUGGGAGGUAGUGG-5'
20-bp ssDNA	5'-CTCCATCACCCTCCATCACC-3'
20-bp dsDNA	5'-CTCCATCACCCTCCATCACC-3'
	3'-GAGGTAGTGGGAGGTAGTGG-5'
20-bp RNA:DNA	5'-CUCCAUCACCCUCCAUCACC-3'
	3'-GAGGTAGTGGGAGGTAGTGG-5'
40-bp ssRNA	5'-UUUCAAUUCCUUUUAGGAUUAAUCUUGAAGAUAGAGUUAA-3'
40-bp dsDNA	5'-TTTCAATTCCTTTTAGGATTAATCTTGAAGATAGAGTTAA-3'
	5'-TTAACTCTATCTTCAAGATTAATCCTAAAAGGAATTGAAA-3'
40-bp dsDNA (3'-overhang)	5'-TTTCAATTCCTTTTAGGATTAATCTTGAAGATAGAGTTAA-3'
	5'-CTTCAAGATTAATCCTAAAAGGAATTGAAATATCTCATAT-3'
40-bp dsRNA (3'-overhang)	5'-UUUCAAUUCCUUUUAGGAUUAAUCUUGAAGAUAGAGUUAA-3'
	5'-CTTCAAGATTAATCCTAAAAGGAATTGAAATATCTCATAT-3'
40-bp dsDNA (5'-overhang)	5'-TTTCAATTCCTTTTAGGATTAATCTTGAAGATAGAGTTAA-3'
	5'-ATTCTCATACTTAAGTGTATCTTCAAGATTAATCCTAAAA-3'
40-bp dsRNA (5'-overhang)	5'-UUUCAAUUCCUUUUAGGAUUAAUCUUGAAGAUAGAGUUAA-3'
	5'-ATTCTCATACTTAAGTGTATCTTCAAGATTAATCCTAAAA-3'

Table 2. HIV-1 specific primers used in qRT-PCR analysis.

Primers	Sequences
Primer 1 Forward ***(R/U5)***	5'-GCCTCAATAAAGCTTGCCTTGA-3'
Primer 1 Reverse ***(R/U5)***	5'-TGACTAAAAGGGTCTGAGGGATCT-3'
Primer 2 Forward	5'-GTAGTGTGTGCCCGTCTGTT-3'
Primer 2 Reverse	5'-TTTCAAGTCCCTGTTCGGGC-3'
Primer 3 Forward	5'-AGAGCGTCGGTATTAAGCGG-3'
Primer 3 Reverse	5'-TGCGAATCGTTCTAGCTCCC-3'
Primer 4 Forward	5'-CTAGAACGATTCGCAGTTAATCCT-3'
Primer 4 Reverse	5'-CTATCCTTTGATGCACACAATAGAG-3'
Primer 5 Forward ***(gag)***	5'-ACTCTAAGAGCCGAGCAAGC-3'
Primer 5 Reverse ***(gag)***	5'-TCTAGTGTCGCTCCTGGTCC-3'
Primer 6 Forward	5'-CTGTTGAGGTGGGGATTTACCA-3'
Primer 6 Reverse	5'-CTGTCCTTTTCTGGCAGCACT-3'
Primer 7 Forward	5'-CCTGGATTCCTGAGTGGGAG-3'
Primer 7 Reverse	5'-TAGTTTCCCTATTGGCTGCCC-3'
Primer 8 Forward	5'-GTCAGCTAAAAGGGGAAGCCA-3'
Primer 8 Reverse	5'-CCACTGGCTACATGAACTGCT-3'
Primer 9 Forward	5'-GAAAGGACCAGCAAAGCTCC-3'
Primer 9 Reverse	5'-CACCTGCCATCTGTTTTCCAT-3'
Primer 10 Forward	5'-TGGAAGCATCCAGGAAGTCAG-3'
Primer 10 Reverse	5'-CCGCTTCTTCCTGCCATAGG-3'
Primer 11 Forward ***(egfp)***	5'-CAACAGCCACAACGTCTATATCATG-3'
Primer 11 Reverse ***(egfp)***	5'-ATGTTGTGGCGGATCTTGAAG-3'
Primer 12 Forward	5'-GCTACAAGGGACTTTCCGCT-3'
Primer 12 Reverse	5'-AGAGAGACCCAGTACAGGCA-3'
Primer 12 Forward	5'-GCTACAAGGGACTTTCCGCT-3'
Primer 12 Reverse	5'-AGAGAGACCCAGTACAGGCA-3'

11. RNA-Seq analysis

Total RNA was extracted from mock- and SAMHD1-expressing U937 cells uninfected or infected with HIV-1 using TRIzol reagent (Invitrogen) by manufacturer's instruction followed by addition of spike-in poly(A)-tailed RNA (GeneChip Eukaryotic Poly-A RNA control Kit, Affymetrix). After ribosomal RNA depletion using Epicentre's Ribo-Zero™ Kits, RNA was fragmented using RNA fragmentation reagent (Ambion). After dephosphorylation by Antarctic phosphatase (NEB), 5' end of fragmented and dephosphorylated RNA was phospho-labeled using [γ-^{32}P]ATP and T4 polynucleotide kinase (TaKaRa). 35-60 nucleotide RNA was extracted in a polyacrylamide, 7 M urea, TBE gel. 3' adaptor (5′/rApp/TGGAATTCTCGGGTGCCAAGG/ddC/-3′, IDT) was ligated using T4 RNA ligase truncated K227Q (NEB) followed by ligation of 5' adaptor (5′ Solexa linker, 100-M; 5′-rGrUrUrCrArGrArGrUrUrCrUrArCrArGrUrCrCrGrA rCrGrA rUrC-3′, IDT) using T4 RNA ligase (TaKaRa). The 5' and 3' adaptor-ligated RNA was reverse transcribed using RNA RT Primer (RTP; 5′-GCCTTG GCACCCGAGAATTCCA-3′, IDT) and SuperScript™ III reverse transcriptase (Invitrogen). Each sample was amplified by PCR using Phusion polymerase (Thermo Scientific), 5′ end Illumina RNA PCR Primer (RP1) and 3′ end Illumina RNA PCR Primer (Index 1-12). RNA-Seq library was sequenced with 51-bp

single-end sequencing in an Illumina HiSeq2500 sequencer. Illumina standard pipeline and software-CASAVA were employed for processing of raw imaging, base calling and generating FASTQ sequence reads. Before aligning reads to the reference sequences, I filtered low quality reads, adapter-containing sequences, and artifact reads using in house software and FASTX-Toolkit (FASTQ/A short-reads pre-processing tools, hannonlab.cshl.edu/fastx toolkit). The read sequences were then aligned to the UCSC hg19 human reference genome and HIV-1 NL4-3 genome using bowtie2-2.1.037. The abundance of transcripts was measured as the score of RPKM (Reads Per Kilobase of exon model per Million mapped reads). I applied spike-in normalization to all 12 samples to reduce variations across samples.

12. RNA immunoprecipitation (RIP)

The RNA immunoprecipitation protocol (62) was adapted to analyze the interactions between SAMHD1 and HIV-1-GFP genomic RNA. HIV-1-GFP-infected cells were cross-linked by 1% formaldehyde for 10 min at room temperature. The crosslinking reaction was stopped by addition of glycine (1 M, pH 7.0) to a final concentration of 0.25 M followed by incubation at room temperature for 5 min. The cells were washed with ice-cold PBS and

resuspended in RIPA buffer (50 mM Tris-HCl, pH 7.4/1% NP40/0.5% sodium deoxycholate/0.05% SDS/1 mM EDTA/150 mM NaCl) containing protease inhibitors and an RNase inhibitor. The cell suspension was sonicated and centrifuged for 10 min at 9000 × g, and the resulting supernatant was pre-cleared by incubation with protein G-agarose beads. The pre-cleared supernatant was incubated with anti-HA or anti-Flag antibody-conjugated beads for 2 h at 4 °C. The beads were washed with RIPA buffer and resuspended with reversal buffer (50 mM Tris-HCl, pH 7.0/5 mM EDTA/10 mM DTT/1% SDS) followed by an incubation for 45 min at 70 °C to reverse the crosslinks. The immunoprecipitated RNAs were isolated according to the manufacturer's protocol (Invitrogen).

13. Northern blot analysis

Approximately one microgram of total RNA was analyzed on a 15% polyacrylamide gel containing 7 M urea after ethidium bromide staining. For Northern blot analysis, an oligomer probe specific for $tRNA^{Lys3}$ (5'-TGGCGCCC GAACAGGGAC-3') (63) was used, which was complementary to 18 nucleotides at the 3' end of $tRNA^{Lys3}$. The RNA in the gel was transferred onto a positively charged nylon membrane by electroblotting at 20 V for 2 h. The

RNA was then cross-linked to the nylon membrane using EDC (1-ethyl-3-(3-dimethylaminopropyl)carbodiimide), and the membrane was baked in an oven at 80 °C overnight. Pre-hybridization and hybridization were subsequently carried out in the presence of ^{32}P-5'-labeled nucleotide probes at 42 °C for 24 h. Following hybridization, the membrane was washed five times in 2x SSC (three times in 2x SSC containing 0.05% SDS and twice in 2x SSC containing 0.1% SDS) before autoradiography.

14. Cell fractionation

For nuclear-cytoplasmic fractionation, monocytes and MDMs were washed in cold PBS and resuspended with lysis buffer (10 mM HEPES, pH 7.9/0.1 mM EDTA/2 mM $MgCl_2$/0.1 mM EGTA/10 mM KCl/0.1 mM DTT/0.5 mM PMSF). NP-40 was added to obtain a final concentration of 1% and mixed by gentle inversion. The cytoplasmic extracts were separated from intact nuclei by low-speed centrifugation at 4 °C and 1400 ×g for 30 sec. The nuclear pellet was resuspended in buffer (20 mM HEPES, pH 7.9/0.1 mM EDTA/0.1 mM EGTA/0.4 M NaCl/1 mM DTT/1 mM PMSF). The nuclear and cytoplasmic fractions were analyzed by immunoblotting.

RESULTS

1. SAMHD1 is a processive 3'-5' exonuclease.

SAMHD1 is a myeloid cell-specific HIV-1 restriction factor that is counteracted by Vpx (4, 5). SAMHD1 possesses a dGTP-dependent dNTPase activity (18, 29), and studies have proposed that SAMHD1 blocks HIV-1 infection by depleting the intracellular dNTP pool (6, 28, 31). Contrary to the proposed role for dNTPase activity in SAMHD1-mediated restriction of HIV-1, recent studies have shown that the phosphorylation of SAMHD1 regulates the ability of this enzyme to restrict HIV-1 infection but does not alter the cellular dNTP levels (32, 33, 64). In addition, SAMHD1 is a nucleic acid binding protein (7, 34, 35) and exhibits a processive exonuclease activity *in vitro* against a broad spectrum of substrates, such as single-stranded DNAs and RNAs as well as the RNA in RNA:DNA hybrids (21). Although the physiological relevance of SAMHD1 nuclease activity remains unknown, SAMHD1 might bind to HIV-1 RNA and degrade this RNA or reverse transcription intermediates.

In contrast to Beloglazova et al.(21), other studies have not observed SAMHD1 nuclease activity (18, 29, 34); therefore, I tested whether SAMHD1 possesses nuclease activity. I incubated purified, full-length, wild-type human SAMHD1 ($SAMHD1_{WT}$) with various types of 20- or 30-mer nucleic acid substrates (Figure 7). $SAMHD1_{WT}$ hydrolyzed both 20- and 30-mer single-

A

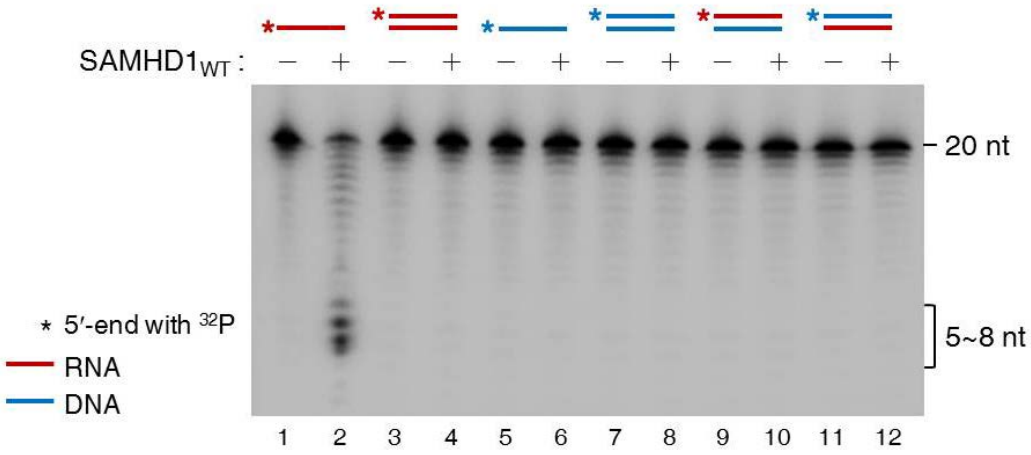
SAMHD1WT : − + − + − + − + − + − +
20 nt
5~8 nt
* 5′-end with 32P
RNA
DNA
1 2 3 4 5 6 7 8 9 10 11 12

B

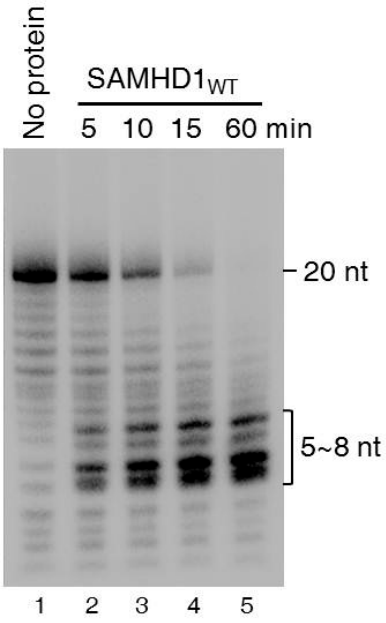
No protein
SAMHD1WT
5 10 15 60 min
20 nt
5~8 nt
1 2 3 4 5

C

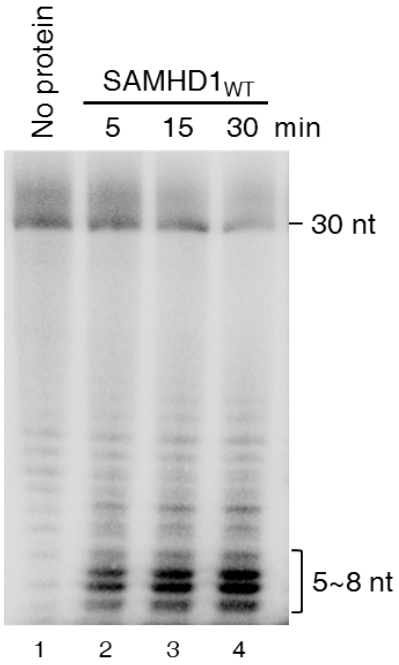
No protein
SAMHD1WT
5 15 30 min
30 nt
5~8 nt
1 2 3 4

Figure 7. SAMHD1 is a ssRNA-specific ribonuclease.

(A) Purified GST-SAMHD1 (150 nM) was incubated for 30 min at 37°C with various synthetic nucleic acid substrates (20-mers) that were 5'-end labeled with [γ-^{32}P]ATP (indicated by an asterisk). The products were analyzed by electrophoresis and autoradiography. RNA and DNA are represented by red and blue lines, respectively. **(B)** GST-SAMHD1 was assayed for ribonuclease activity in time course experiments. The ribonuclease activity was determined using a 20-mer ssRNA as substrate by measuring and quantifying the disappearance of the substrate. **(C)** An RNase activity assay performed as described in (A) using 30-mer ssRNA substrates.

stranded RNAs (ssRNA), releasing 5'-mononucleotides and leaving a short undigested 5~8-mer core. To characterize the ribonuclease function of SAMHD1 more precisely, SAMHD1 was incubated for different periods of time with a 20-mer ssRNA. This incubation resulted in the loss of the substrate and in the accumulation of 5~8-mer final products with a direct substrate/product relationship. The specific activity of SAMHD1 was 58.5±0.81 $pmol \cdot min^{-1} \cdot nmol^{-1}$ (Figure 7B). This value is comparable with that reported for eukaryotic exoribonuclease RNase R (65). No fragments of intermediate length were observed (Figure 7B and C), which is a distinct feature of a processive rather than a distributive mode of hydrolysis.

No nuclease activity was detected on dsRNA, ssDNA, dsDNA, and RNA-DNA hybrid substrates, whereas these substrates were digested by positive control nucleases (Figure 8). Essentially identical results were obtained when the experiments were repeated using the 40-mer nucleic acid substrates described by Beloglazova et al. (21) (Figure 9). A previous study (21) observed that SAMHD1 degrades ssRNA, ssDNA, RNA in RNA:DNA hybrids, and the *in vitro*-transcribed HIV-1 RNA fragments; however, I observed that only ssRNAs, including *in vitro*-HIV-1 transcripts in the size range of 336 to 593 nucleotides (Figure 10), were sensitive to SAMHD1 digestion. These discrepancies might be due to differences in assay conditions or protein purification procedures;

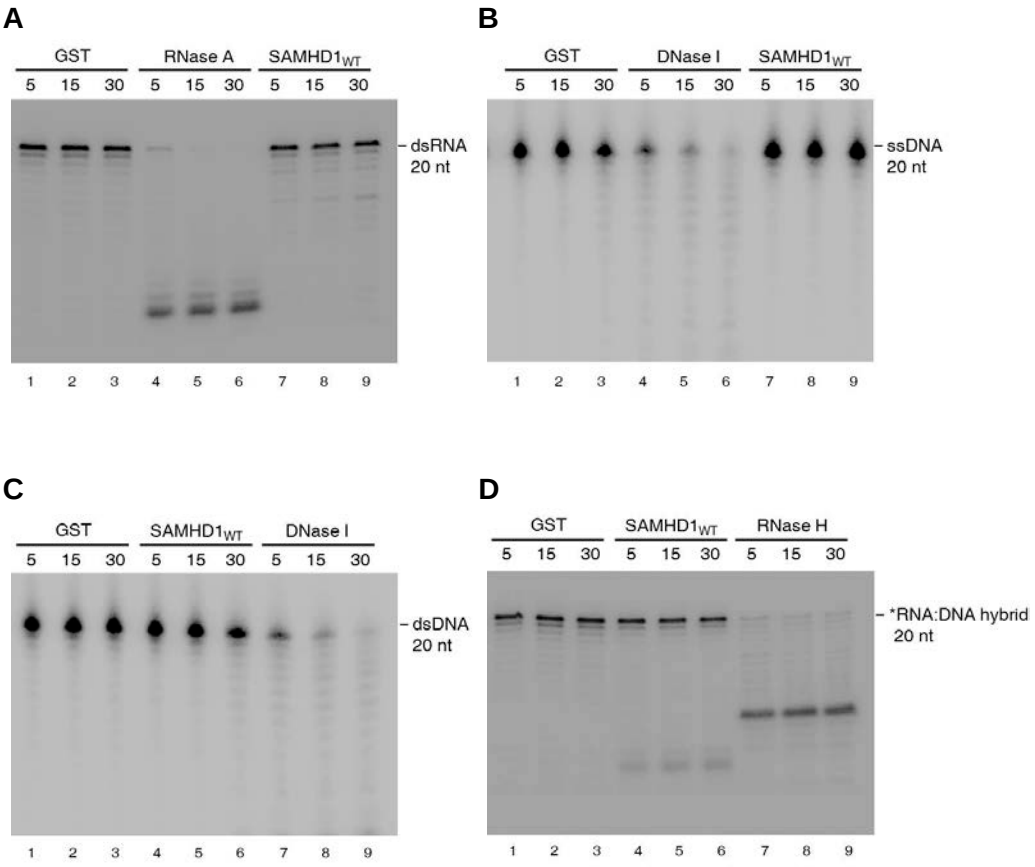
A
GST
RNase A
SAMHD1WT
5 15 30 5 15 30 5 15 30
dsRNA
20 nt
1 2 3 4 5 6 7 8 9
B
GST
DNase I
SAMHD1WT
5 15 30 5 15 30 5 15 30
ssDNA
20 nt
1 2 3 4 5 6 7 8 9
C
GST
SAMHD1WT
DNase I
5 15 30 5 15 30 5 15 30
dsDNA
20 nt
1 2 3 4 5 6 7 8 9
D
GST
SAMHD1WT
RNase H
5 15 30 5 15 30 5 15 30
*RNA:DNA hybrid
20 nt
1 2 3 4 5 6 7 8 9

Figure 8. Nuclease activity of SAMHD1 compared to other enzymes.

Various types of 20-mer nucleic acid substrates were incubated with GST-SAMHD1 (150 nM) and analyzed for nuclease activity of SAMHD1, as in Figure 7. RNase A, DNase I and RNase H were used as positive nuclease controls toward dsRNA, ssDNA/dsDNA and RNA:DNA hybrid substrates, respectively.

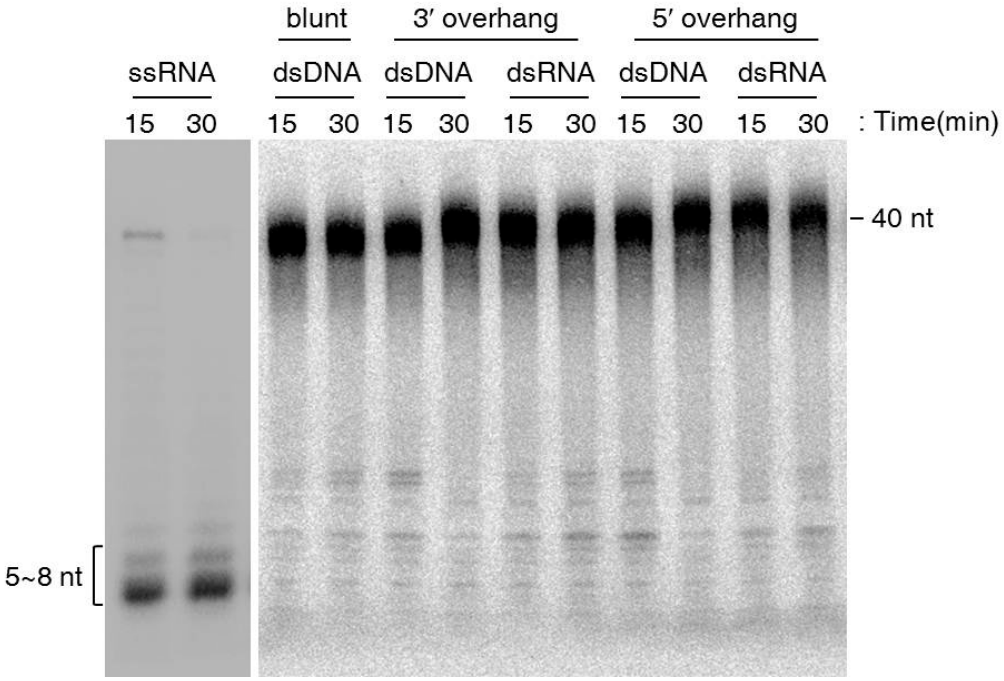
blunt
3′ overhang
5′ overhang
ssRNA
dsDNA
dsDNA
dsRNA
dsDNA
dsRNA
15 30 15 30 15 30 15 30 15 30 15 30
: Time(min)
– 40 nt
5~8 nt

Figure 9. Nuclease activity of SAMHD1 with 40-nt nucleic acid substrates.

Various types of 40-mer nucleic acid substrates (50 nM) with 5' or 3' overhangs or blunt ends were 5'-end labeled with [γ-^{32}P]ATP and incubated with purified GST-SAMHD1 (150 nM) for 15 and 30 min at 37 °C. The products were analyzed by electrophoresis and autoradiography.

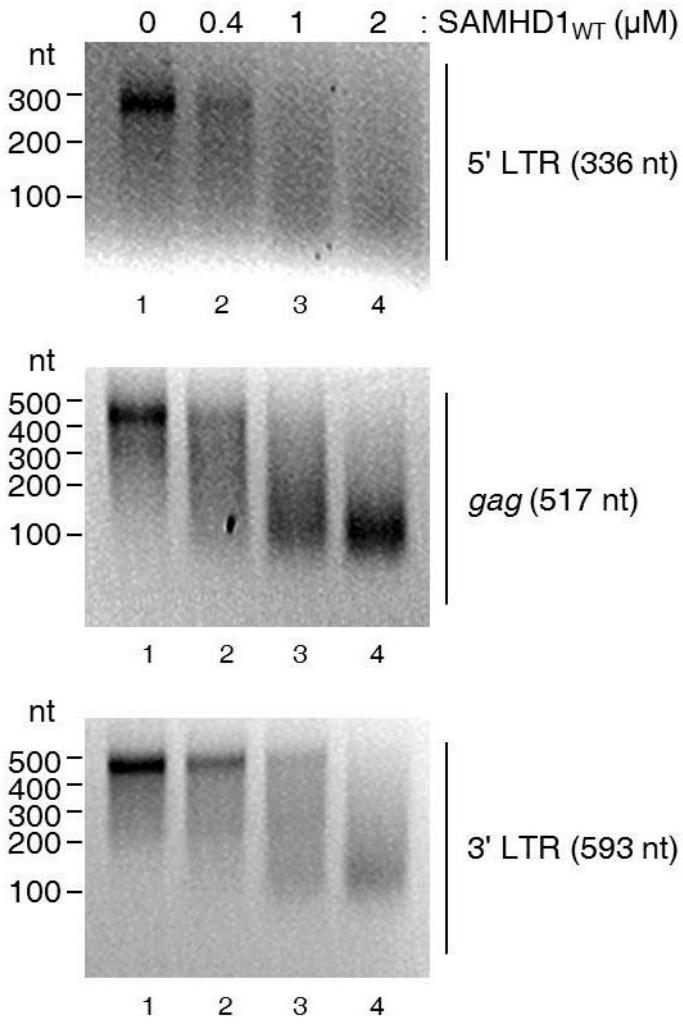
0 0.4 1 2 : SAMHD1WT (μM)
nt
300
200
100
5' LTR (336 nt)
1 2 3 4
nt
500
400
300
200
100
gag (517 nt)
1 2 3 4
nt
500
400
300
200
100
3' LTR (593 nt)
1 2 3 4

Figure 10. SAMHD1 cleaves *in vitro*-transcribed HIV-1 RNAs.

In vitro transcripts of HIV-1 5' LTR (336 bases), gag (517 bases), and 3' LTR (593 bases) RNAs were synthesized using a T7 RNA polymerase transcription kit. These RNA substrates (0.2 μM) were incubated with GST-SAMHD1 (0.4, 1, and 2 μM) at 37 °C for 1 h. The reaction products were analyzed by electrophoresis in a 2% agarose gel and visualized by ethidium bromide staining.

however, my results are consistent with the observation of Beloglazova et al. (21) that SAMHD1 cleaves ssRNAs processively *in vitro*.

Next, to determine the direction of the degradation of ssRNA, SAMHD1 was incubated with another 30-mer ssRNA labeled with ^{32}P at its 3'-end instead of its 5' -end. This incubation led to the loss of the signal, with no intermediate, and the signal of one nucleotide size was increased (Figure 11A). By contrast, the substrate with a phosphate group at its 3'-end was not degraded (Figure 11B). These results show that the SAMHD1-mediated degradation of ssRNA occurs in the 3' to 5' direction and displays a strong preference for a 3'-end containing a free hydroxyl group. The degradation of ssRNA by SAMHD1 required Mg^{2+} (Figure 12) and correlated with the presence of the $SAMHD1_{WT}$ protein across chromatographic fractions (Figure 13). Considering the preferential binding of SAMHD1 to ssRNA compared with ssDNA (34, 35) and the absence of an interaction between endogenous SAMHD1 and dsRNA, dsDNA or RNA:DNA hybrids (35), I concluded that SAMHD1 is an RNase that digests ssRNA.

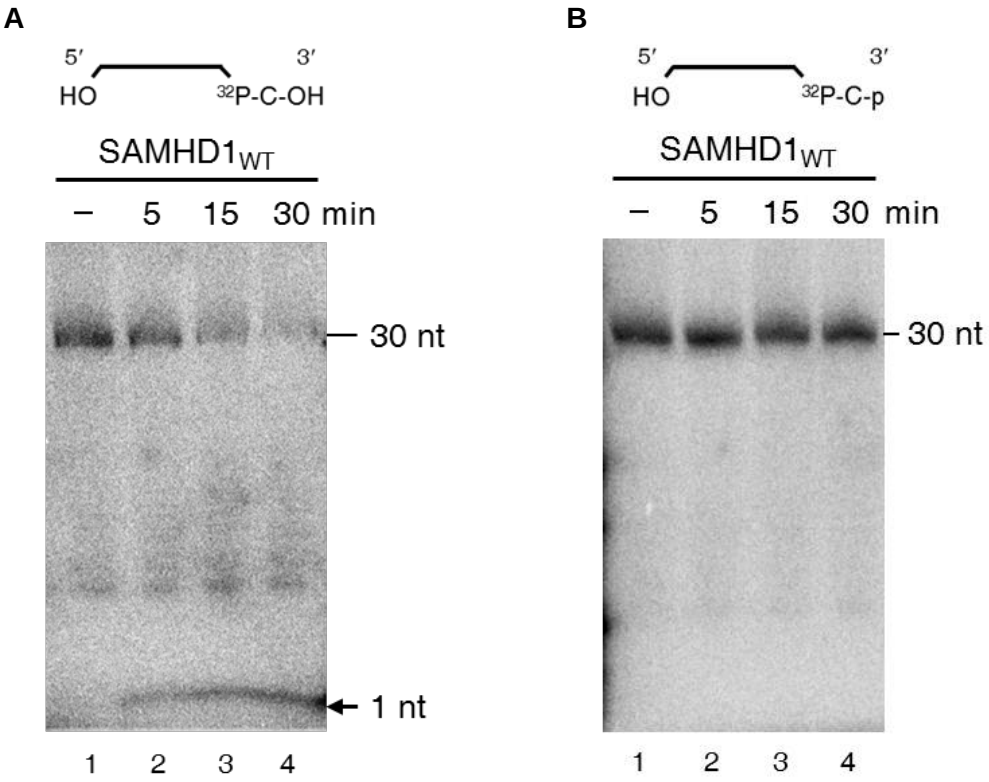
A
5′
3′
HO
32P-C-OH
SAMHD1WT
–
5
15
30 min
30 nt
1 nt
1
2
3
4
B
5′
3′
HO
32P-C-p
SAMHD1WT
–
5
15
30 min
30 nt
1
2
3
4

Figure 11. SAMHD1 degrades RNA with a preference for a 3'-end containing a free hydroxyl group in a 3' to 5' direction.

GST-SAMHD1 was assayed for exoribonuclease activity in time course experiments. The RNA substrates were labeled with ^{32}P at 3'-end. The 3'-end of the 30-mer substrate carried a hydroxyl group **(A)** or a phosphate group **(B)**. The reaction products were separated by PAGE and visualized by autoradiography.

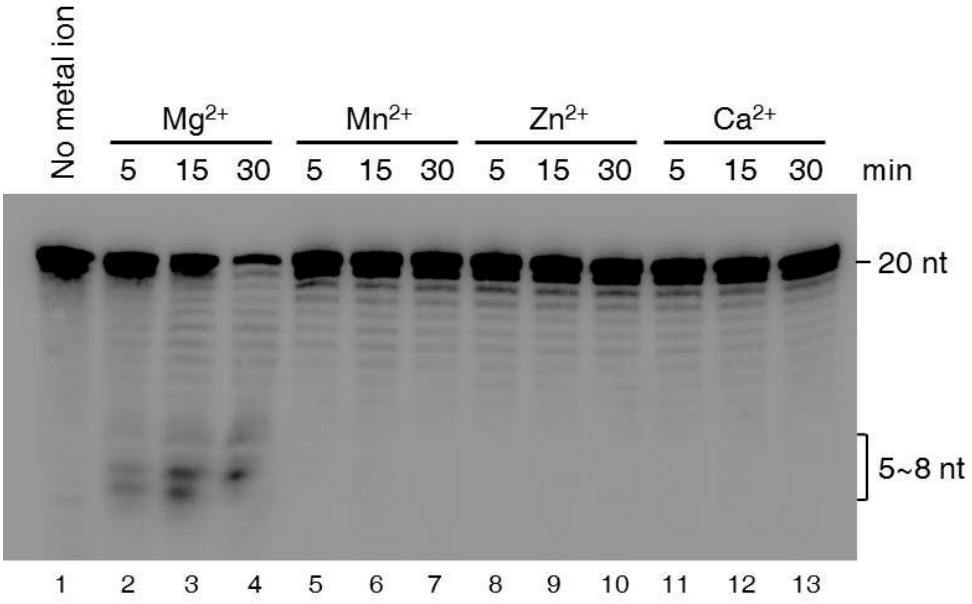
No metal ion
Mg2+
Mn2+
Zn2+
Ca2+
5 15 30 5 15 30 5 15 30 5 15 30 min
20 nt
5~8 nt
1 2 3 4 5 6 7 8 9 10 11 12 13

Figure 12. Metal specificity of SAMHD1.

5'-end ^{32}P-labeled ssRNA (20-mer) was incubated with GST-SAMHD1 (150 nM) without added metal or with 5 mM Mg^{2+}, Mn^{2+}, Zn^{2+}, or Ca^{2+}. The reaction products were analyzed by PAGE and autoradiography.

A

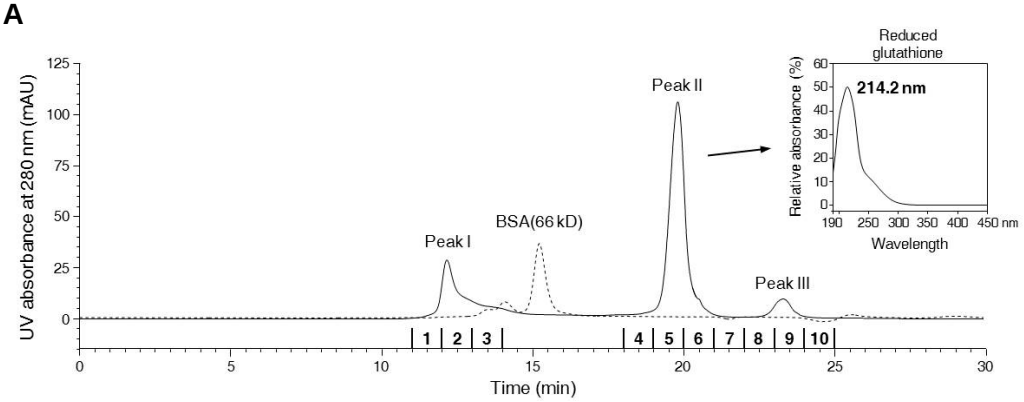
UV absorbance at 280 nm (mAU)
125
100
75
50
25
0
Peak I
BSA(66 kD)
Peak II
Peak III
1
2
3
4
5
6
7
8
9
10
0
5
10
15
20
25
30
Time (min)
Reduced glutathione
214.2 nm
Relative absorbance (%)
60
50
40
30
20
10
0
190
250
300
350
400
450 nm
Wavelength

B

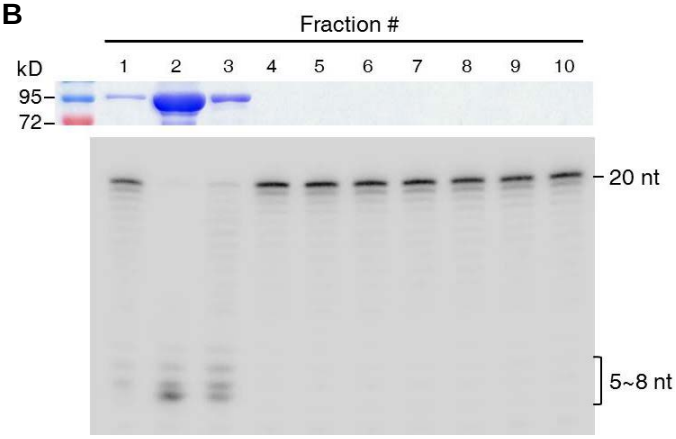
Fraction #
kD
1
2
3
4
5
6
7
8
9
10
95
72
20 nt
5~8 nt

Figure 13. Correlation of the presence of the SAMHD1$_{WT}$ protein with RNase activity.

Recombinant GST-tagged SAMHD1 was expressed in *E. coli* Rosetta cells and purified using glutathione-Sepharose column chromatography. The resulting eluate was further purified by a size-exclusion column (YMC-Pack Diol-200). **(A)** HPLC chromatograms of the resulting eluate and BSA molecular weight standards (dotted line, Mr≈66 kD). Inset, UV spectrum of the peak at 19.8 min corresponding to reduced co-eluted glutathione. **(B)** 10 fractions corresponding to peaks I, II, and III were collected, stained with Coomassie Blue and assayed for RNase activity using 5'-end ^{32}P-labeled ssRNA (20-mer) as a substrate.

2. Ribonuclease and dNTPase are dual and separate functions of SAMHD1.

The dNTPase function of SAMHD1 is allosterically activated by dGTP. Mutations of Asp 137 and Arg 145 in the allosteric site or Asp 207 and Asp 311 in the catalytic site in the HD domain abolish dNTPase activity entirely (18, 29). Unlike dNTPase activity, RNase activity does not require the cofactor dGTP (Figure 7); therefore, I proposed that these two catalytic functions of SAMHD1 might be physically separable. I characterized AGS-associated SAMHD1 mutations and mutations near the allosteric dGTP-binding sites for defects in RNase or dNTPase activity and identified several point mutations that caused loss of function. Mutations at amino acids 207 and 311 in the catalytic site abolished both RNase and dNTPase activities (Figure 14). A mutation at residue D137 in the allosteric site ($SAMHD1_{D137N}$) had no effect on the RNase activity but did abolish the dNTPase activity (Figure 14), whereas the AGS-mutant $SAMHD1_{Q548A}$ showed the opposite phenotype. Due to the relative insolubility of GST-$SAMHD1_{Q548A}$ proteins in *E. coli*, we used $SAMHD1_{Q548A}$ proteins immunoprecipitated from U937 monocytic cells. Unlike the processive degradation seen in $SAMHD1_{WT}$ and $SAMHD1_{D137N}$, the Q548A mutation caused the enzyme to digest ssRNA in a distributive manner featured by

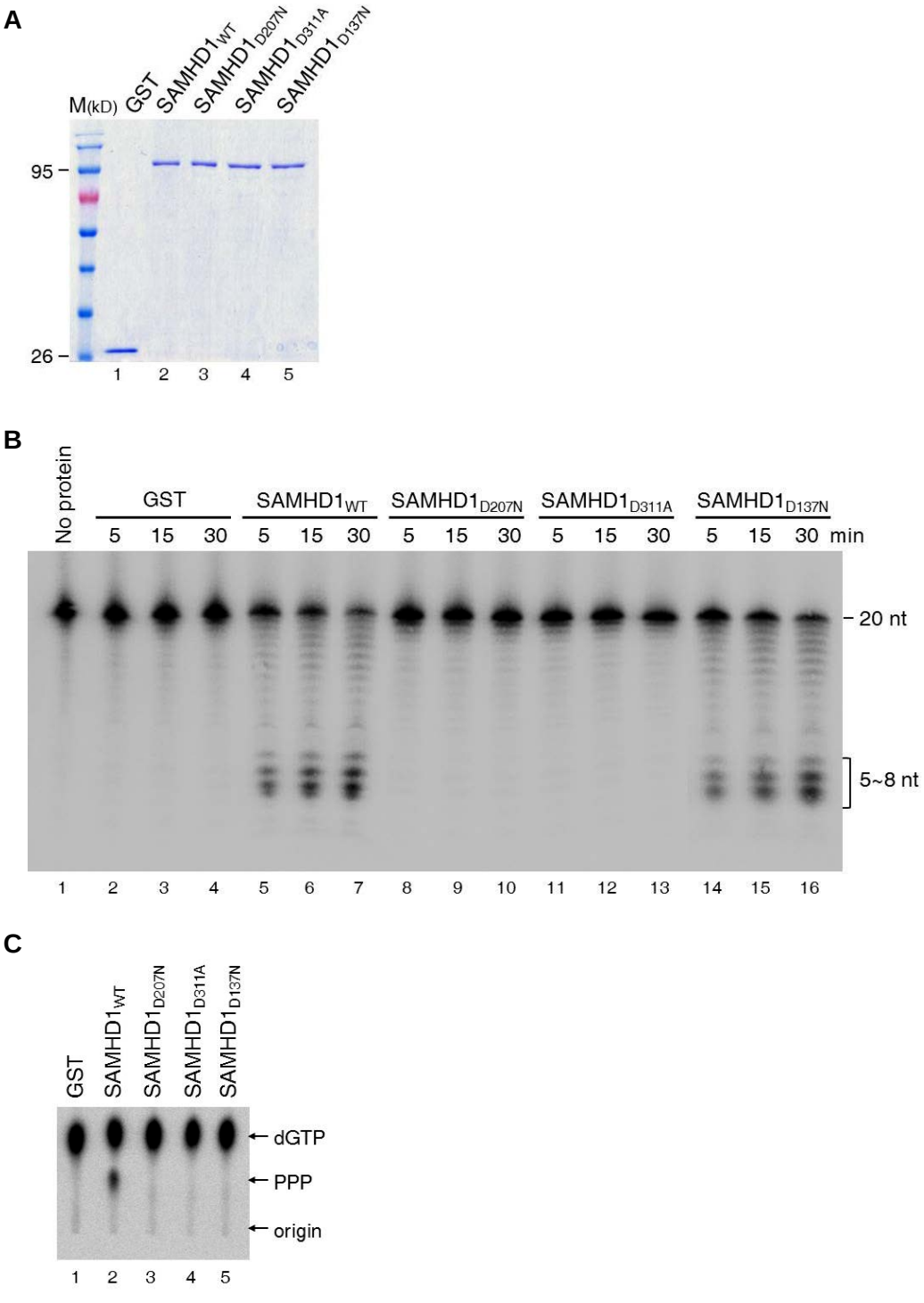
A
M(kD)
GST
SAMHD1WT
SAMHD1D207N
SAMHD1D311A
SAMHD1D137N
95
26
1 2 3 4 5
B
No protein
GST
SAMHD1WT
SAMHD1D207N
SAMHD1D311A
SAMHD1D137N
5 15 30 5 15 30 5 15 30 5 15 30 5 15 30 min
20 nt
5~8 nt
1 2 3 4 5 6 7 8 9 10 11 12 13 14 15 16
C
GST
SAMHD1WT
SAMHD1D207N
SAMHD1D311A
SAMHD1D137N
dGTP
PPP
origin
1 2 3 4 5

Figure 14. Identification of amino acid residues required for RNase activity or dNTPase activity of SAMHD1.

(A) Recombinant GST-fusion SAMHD1 was expressed in *E. coli* Rosetta cells and purified using glutathione-Sepharose column chromatography. Approximately 1 μg of indicated proteins were subjected to 10% SDS-PAGE, and the gel was stained with Coomassie Blue. The molecular weight standards (lane 1) are indicated. **(B)** An RNase activity assay performed for SAMHD1 mutants as described in Figure 7 using 20-mer ssRNA substrates. **(C)** A dGTP-triphosphohydrolase assay was performed for GST-SAMHD1 variants as described previously.

accumulation of intermediate-size fragments (16–19 nucleotides) (Figure 15). Considering that a shift from a processive to distributive degradation often occurs under the conditions that decrease the affinity of an exonuclease for its substrates (66, 67), this switch in mode may be because of a lowered affinity of $SAMHD1_{Q548A}$ for ssRNA. Indeed, recent studies have shown that $SAMHD1_{Q548A}$ exhibits impaired ssRNA binding (21, 35). Notably, dGTP inhibited the RNase activity of SAMHD1 on ssRNA substrates, and this inhibition correlated with a shift from a processive to a distributive mode of action (Figure 16), suggesting that dGTP interferes with the binding of SAMHD1 to the substrates.

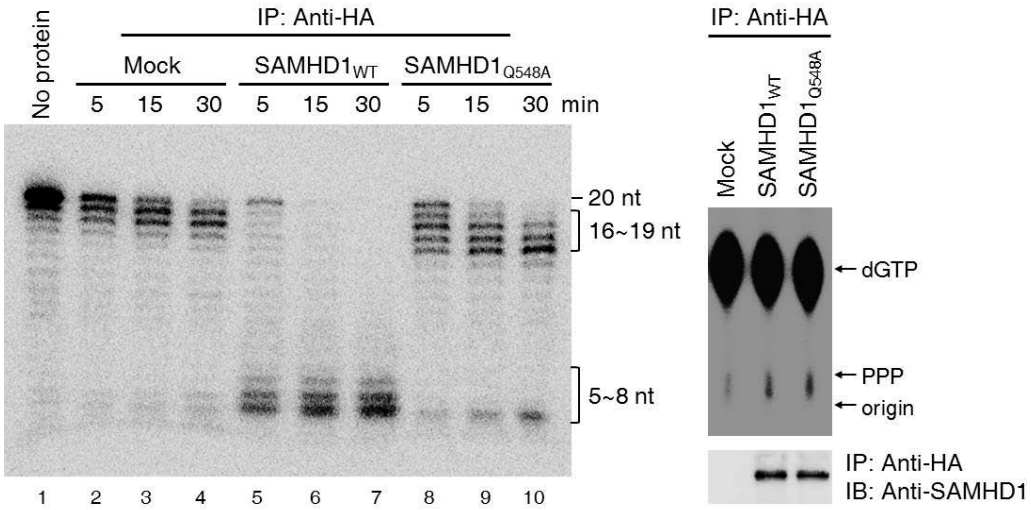
No protein
IP: Anti-HA
Mock
SAMHD1WT
SAMHD1Q548A
5 15 30 5 15 30 5 15 30 min
20 nt
16~19 nt
5~8 nt
1 2 3 4 5 6 7 8 9 10
IP: Anti-HA
Mock
SAMHD1WT
SAMHD1Q548A
dGTP
PPP
origin
IP: Anti-HA
IB: Anti-SAMHD1

Figure 15. Q548 residue of SAMHD1 is important for RNase activity not for dNTPase activity.

The HA-tagged $SAMHD1_{WT}$ and $SAMHD1_{Q548A}$ proteins were purified from the PMA-differentiated U937 cells using anti-HA antibody. An RNase and a dGTP triphosphohydrolase assays were performed as described in Figure 14. IP, immunoprecipitation: IB, immunoblot.

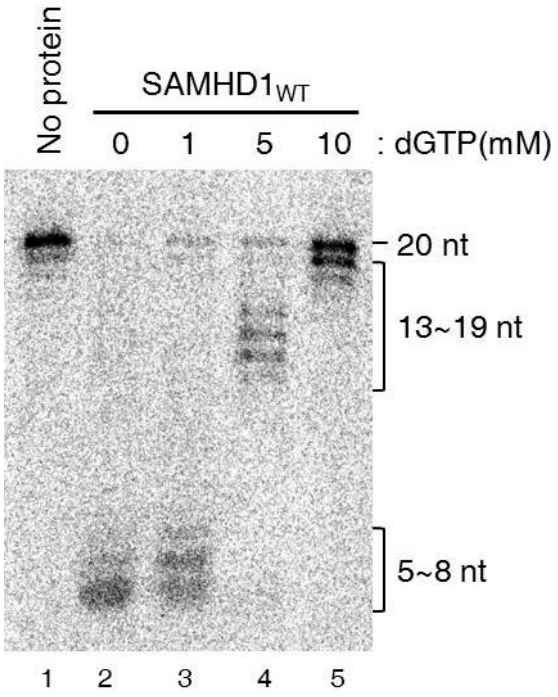
No protein
SAMHD1WT
0 1 5 10 : dGTP(mM)
20 nt
13~19 nt
5~8 nt
1 2 3 4 5

Figure 16. dGTP inhibits the RNase activity of SAMHD1.

5'-end ^{32}P-labeled ssRNA (20-mer) was incubated with GST-SAMHD1 (150 nM) in the presence of dGTP (1, 5, 10 mM) at 37 °C for 30 min. GST-SAMHD1 was preincubated with dGTP for tetramerization. Reaction products were analyzed by PAGE and autoradiography.

3. The ribonuclease function of SAMHD1 is critical for HIV-1 restriction.

The identification of the $SAMHD1_{D137N}$ and $SAMHD1_{Q548A}$ mutants that retain only one of two enzymatic activities enabled me to determine the discrete contribution of SAMHD1 RNase activity to HIV-1 restriction. For this analysis, I stably expressed wild-type SAMHD1 or each of the SAMHD1 mutants in U937 human pro-monocytic cells, which do not express endogenous SAMHD1 and can be differentiated to macrophage-like cells by PMA treatment to enable them support HIV-1 replication (4, 28, 32, 33). The wild-type and mutant proteins were expressed at comparable levels (Figure. 15A). Consistent with *in vitro* data (Figure 14), the catalytic mutants ($SAMHD1_{D207N}$ and $SAMHD1_{D311A}$) and the allosteric mutant ($SAMHD1_{D137N}$) did not reduce the intracellular levels of dNTPs, whereas $SAMHD1_{Q548A}$ decreased the cellular levels of dNTPs (Figure 17B). $SAMHD1_{WT}$ effectively inhibited HIV-1 infection, whereas the catalytically defective $SAMHD1_{D207N}$ and $SAMHD1_{D311A}$ proteins did not restrict HIV-1 infection. Notably, $SAMHD1_{D137N}$ restricted HIV-1 infection to nearly the same extent as $SAMHD1_{WT}$. $SAMHD1_{Q548A}$ was unable to block HIV-1 restriction despite its ability to decrease the cellular levels of dNTPs (Figure 18). These data suggest that the RNase but not the dNTPase

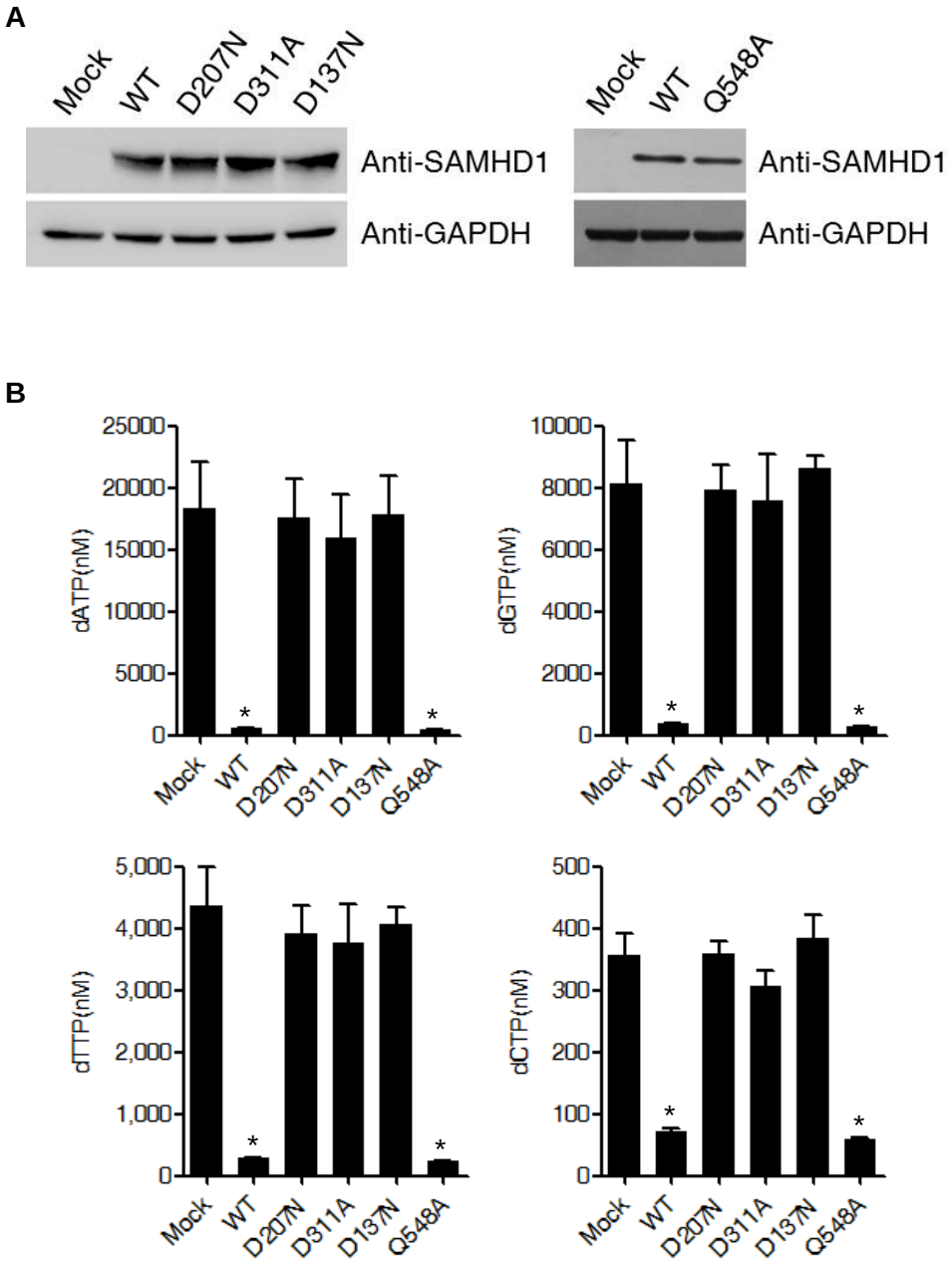
A
Mock
WT
D207N
D311A
D137N
Anti-SAMHD1
Anti-GAPDH
Mock
WT
Q548A
Anti-SAMHD1
Anti-GAPDH
B
dATP(nM)
25000
20000
15000
10000
5000
0
dGTP(nM)
10000
8000
6000
4000
2000
0
dTTP(nM)
5,000
4,000
3,000
2,000
1,000
0
dCTP(nM)
500
400
300
200
100
0
*
Mock
WT
D207N
D311A
D137N
Q548A

Figure 17. The intracellular dNTP pools were measured in U937 cells stably expressing SAMHD1 variants.

(A) Expression level of SAMHD1 variants in U937 cells. U937 cell lines stably expressing SAMHD1 variants were generated by using retroviral vector. Cells were treated with PMA (30 ng/ml) for 20 h and lysed. The cell extracts were immunoblotted to verify the expression of SAMHD1. GAPDH serves as a loading control. **(B)** Quantification of dNTPs from U937 cell lines stably expressing SAMHD1 variants. The data are presented as the mean ± s.d. of triplicate independent experiments. (* indicates significant differences compared with the mock-transfected control at $P < 0.05$ using the two-tailed Student's t test).

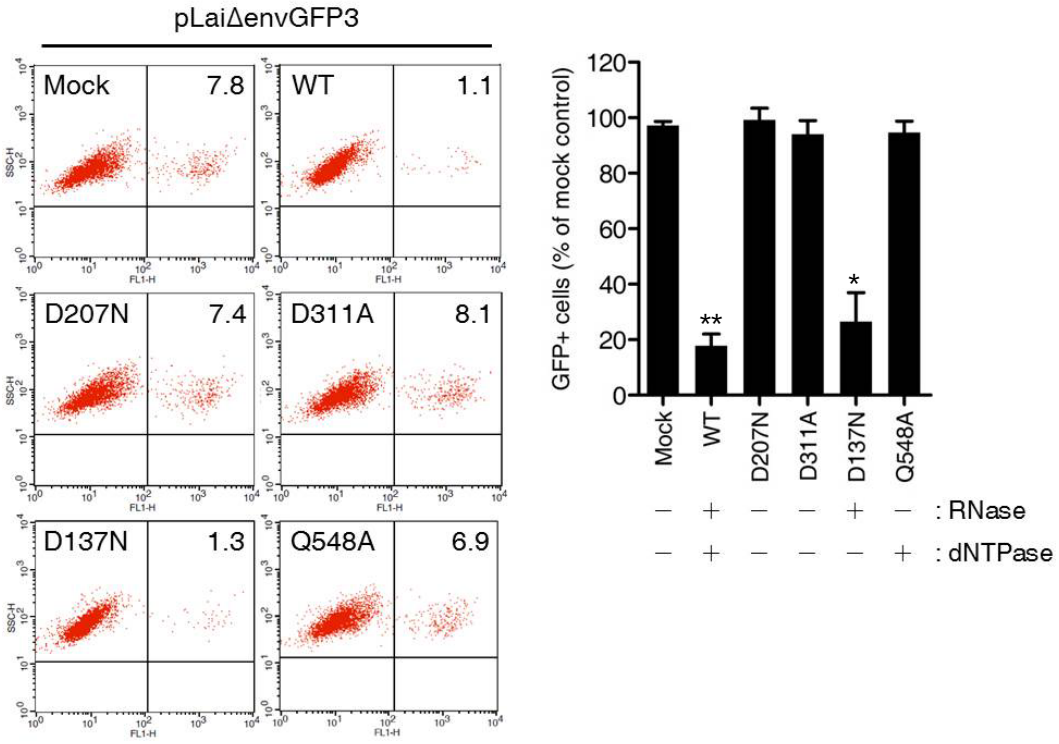
pLaiΔenvGFP3
Mock
7.8
WT
1.1
D207N
7.4
D311A
8.1
D137N
1.3
Q548A
6.9
SSC-H
FL1-H
GFP+ cells (% of mock control)
120
100
80
60
40
20
0
**
*
Mock
WT
D207N
D311A
D137N
Q548A
− + − − + − : RNase
− + − − − + : dNTPase

Figure 18. The RNase but not the dNTPase function of SAMHD1 is required for HIV-1 restriction.

U937 cells stably expressing SAMHD1 mutants were treated with PMA and infected by pLaiΔenvGFP3, a HIV-1-GFP reporter virus with the LAI backbone. After 48 h, the percentages of GFP-positive cells were analyzed using flow cytometry. The percentage of GFP-positive cells was calculated relative to the number of GFP-positive mock-transfected cells. The data are presented as the mean ± s.d. of triplicate independent experiments. (* and ** indicate significant differences compared with the mock-transfected control at $P < 0.05$ and $P < 0.001$, respectively, using the two-tailed Student's t test).

function of SAMHD1 is essential for HIV-1 restriction. The quantification of viral cDNA intermediates by quantitative PCR using primers specific to different stages of HIV-1 reverse transcription showed that $SAMHD1_{D137N}$ inhibited the synthesis of both the early and late viral cDNA products at a level comparable to $SAMHD1_{WT}$ (Figure 19), indicating that SAMHD1 RNase functions at the early step of HIV-1 reverse transcription.

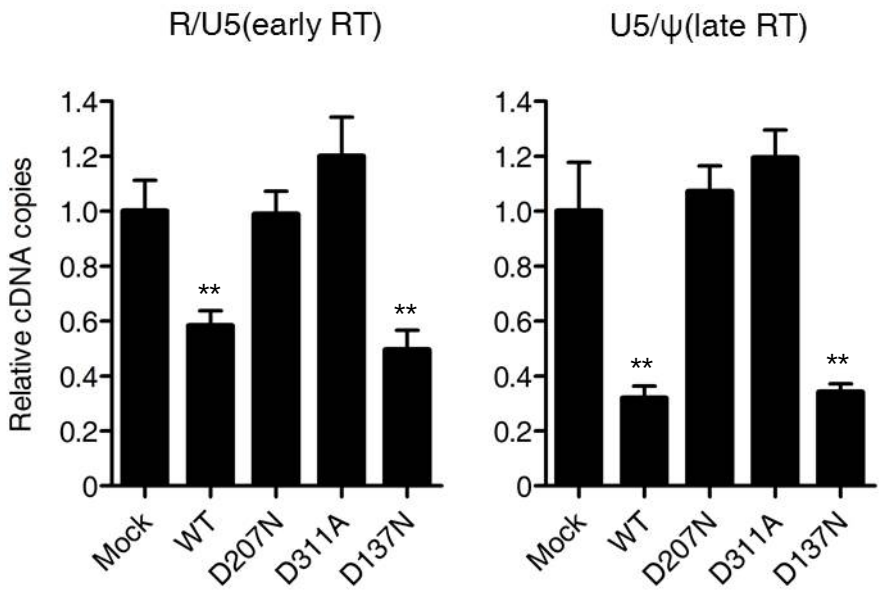
R/U5(early RT)
U5/ψ(late RT)
Relative cDNA copies
1.4
1.2
1.0
0.8
0.6
0.4
0.2
0
**
**
**
**
Mock
WT
D207N
D311A
D137N

Figure 19. SAMHD1 RNase functions at the early step of HIV-1 reverse transcription.

The synthesis of viral cDNA intermediates was determined 24 h after infection by qPCR using the R/U5 (early products) and U5/ψ (late products) primers. Isolated RNAs were treated with DNase I to remove the potential DNA contaminants prior to qPCR analysis and the data were normalized to an internal control gene (*MDM2*). The data are presented as the mean ± s.d. of triplicate independent experiments. (** indicates significant differences compared with the mock-transfected control at $P < 0.001$ using the two-tailed Student's t test).

4. SAMHD1 associates with and induces destabilization of the HIV-1 genomic RNA.

I studied the mechanism by which SAMHD1 RNase activity inhibits HIV-1 replication. HIV-1 reverse transcription involves two RNA components: the $tRNA^{Lys3}$ primer and the HIV-1 genomic RNA, which is a template for cDNA synthesis. The experimental design is outlined in Figure 20A. Total cellular RNA was isolated from U937 cells infected with HIV-1-GFP at the early time points post-infection. Northern blot analysis revealed that SAMHD1 had no effect on $tRNA^{Lys3}$ levels (Figure 20B). I tested whether SAMHD1 RNase activity affects HIV-1 RNA levels. The quantification of viral RNA content by quantitative reverse transcription-PCR (qRT-PCR) showed that HIV-1 genomic RNA was significantly reduced in cells expressing $SAMHD1_{WT}$ or $SAMHD1_{D137N}$ at 3 and 6 h post-infection (h.p.i) (Figure 21), but $SAMHD1_{D207N}$, $SAMHD1_{D311A}$, and $SAMHD1_{Q548A}$ did not reduce the level of HIV-1 genomic RNA; these results were consistent with FACS analyses (Figure 18). At 1 h.p.i, both $SAMHD1_{WT}$ and $SAMHD1_{D137N}$ had no impact on the viral RNA content (Figure 21) most likely because the HIV-1 genomic RNA is inaccessible to SAMHD1 at this early time. To exclude primer-specificity bias, 12 pairs of primers spanning the entire HIV-1 genomic RNA region were used to amplify fragments from

A

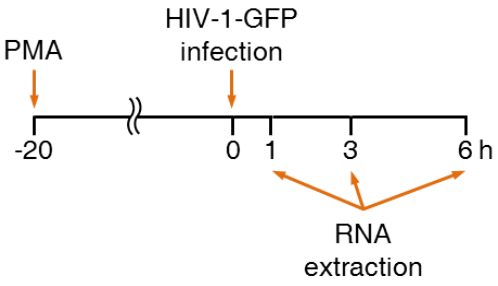
PMA
HIV-1-GFP
infection
-20
0
1
3
6 h
RNA
extraction

B

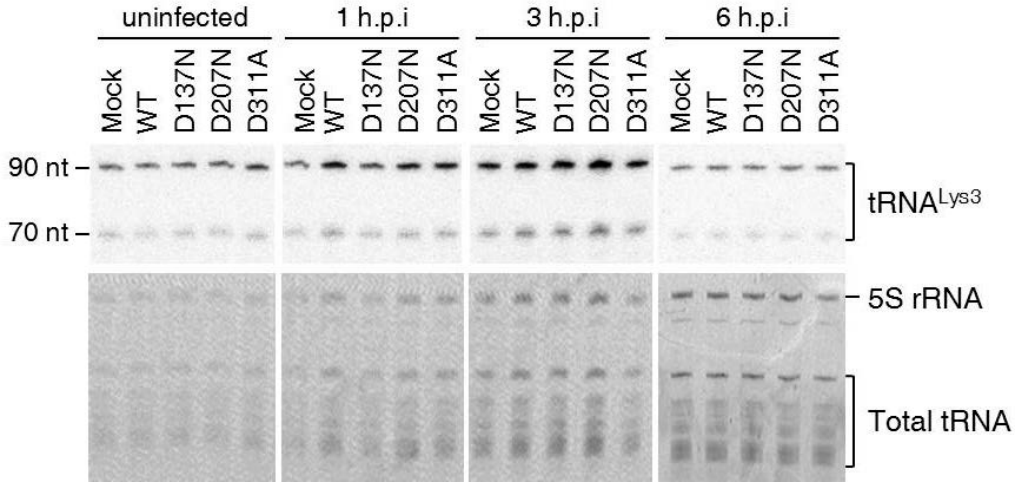
uninfected
1 h.p.i
3 h.p.i
6 h.p.i
Mock
WT
D137N
D207N
D311A
90 nt –
70 nt –
tRNA^{Lys3}
5S rRNA
Total tRNA

Figure 20. SAMHD1 had no effect on $tRNA^{Lys3}$ levels.

(A) The experimental design for time course analysis. SAMHD1-expressing U937 cells were infected with HIV-1-GFP and total cellular RNA was extracted at different time points post-infection. **(B)** Northern blot analysis of $tRNA^{Lys3}$ levels using 18-mer nucleotide probe specific for $tRNA^{Lys3}$ as a probe. Equal loading of RNA samples is shown by ethidium bromide stain of gel before Northern blotting.

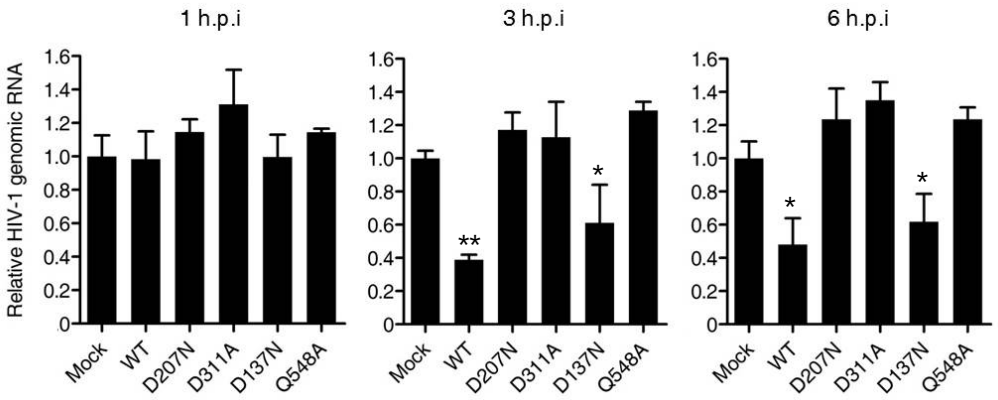
1 h.p.i
3 h.p.i
6 h.p.i
Relative HIV-1 genomic RNA
1.6
1.4
1.2
1.0
0.8
0.6
0.4
0.2
0
**
*
*
*
Mock
WT
D207N
D311A
D137N
Q548A

Figure 21. The level of HIV-1 genomic RNA was decrease in SAMHD1-expressing cells during infection.

The total cellular RNA was extracted from SAMHD1-expressing, HIV-1-GFP-infected U937 cells. The HIV-1 RNA content was quantified by qRT-PCR using HIV-1 *gag*-specific primers. The data were normalized to an internal β-actin. (* and ** indicate significant differences compared with the mock-transfected control at $P < 0.05$ and $P < 0.001$, respectively, using the two-tailed Student's t test).

HIV-1-infected cells. At 3 and 6 h.p.i, the HIV-1 genomic RNA level in $SAMHD1_{WT}$-expressing cells was distinctly lower compared with the mock-transfected control cells (Figure 22). During reverse transcription, the RNase H activity of the viral RT degrades the HIV-1 genomic RNA. To exclude the effect of the viral RT RNase H activity on the HIV-1 genomic RNA level, I used RNase H-defective HIV-1 ($HIV\text{-}1_{D443N}$) in which the amino acid Asp 443 of RT was mutated to Asn (D443N) (68). The level of $HIV\text{-}1_{D443N}$ RNA was lower in $SAMHD1_{WT}$-expressing cells compared with mock-transfected cells (Figure 23), indicating that SAMHD1 can degrade HIV-1 RNA in the absence of reverse transcription.

RNA-Seq analysis also confirmed the degradation of HIV-1 genomic RNA by SAMHD1. Total RNA was extracted 0, 1, and 3 h.p.i from mock or mutant SAMHD1-expressing U937 cells uninfected or infected with HIV-1. I applied a spike-in normalization for all 12 samples to reduce background noise and allow comparison between samples. At 3 h.p.i, the relative read count of HIV-1 genomic RNA in $SAMHD1_{WT}$ and $SAMHD1_{D137N}$-expressing cells was lower than that in mock-transfected or $SAMHD1_{D207N}$-expressing cells despite the considerable reduction of HIV-1 genomic RNA levels in all cell types compared with the levels observed at 1 h.p.i (Figure 24A and B). The relative $tRNA^{Lys3}$-specific read count was comparable among all cell types (Figure 24C). shRNA-

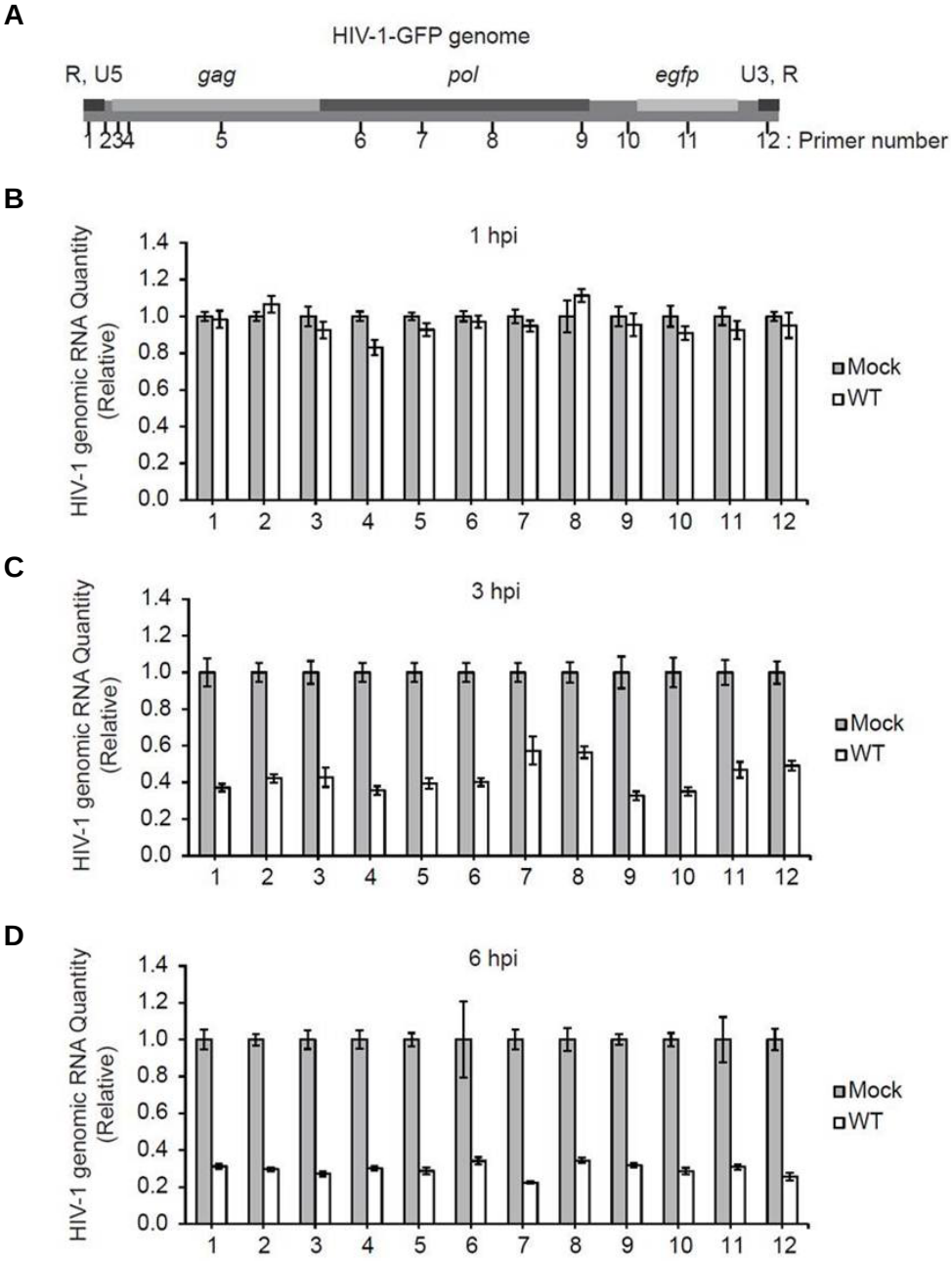
A
HIV-1-GFP genome
R, U5
gag
pol
egfp
U3, R
1 2 3 4 5 6 7 8 9 10 11 12 : Primer number
B
1 hpi
HIV-1 genomic RNA Quantity (Relative)
Mock
WT
C
3 hpi
HIV-1 genomic RNA Quantity (Relative)
Mock
WT
D
6 hpi
HIV-1 genomic RNA Quantity (Relative)
Mock
WT

Figure 22. SAMHD1 degrades multiple regions of the HIV-1 genomic RNA during infection.

(A) HIV-1 genomic amplification sites of the qRT-PCR primers used in (B), (C), and (D). **(B-D)** U937 cells stably expressing empty vector or wild-type (WT) SAMHD1 protein were infected with HIV-1-GFP, and total cellular RNA was extracted at 1 (B), 3 (C), and 6 h.p.i (D). The HIV-1 genomic RNA levels were analyzed by qRT-PCR using site-specific primers corresponding to multiple regions, as indicated in (A). The data were normalized to the GAPDH mRNA levels and compared with the relative level in mock-transfected U937 cells. The data are presented as the means ± s.e.m. of triplicate independent experiments.

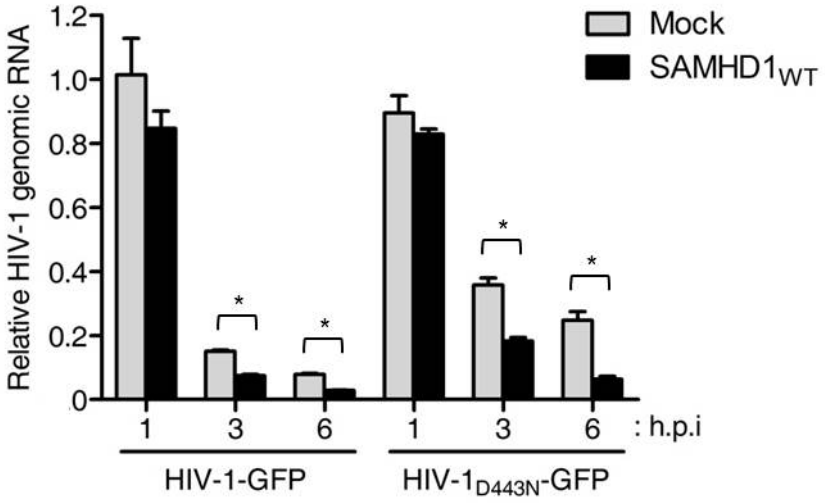
Relative HIV-1 genomic RNA
1.2
1.0
0.8
0.6
0.4
0.2
0
Mock
SAMHD1WT
*
*
*
*
1
3
6
1
3
6
: h.p.i
HIV-1-GFP
HIV-1D443N-GFP

Figure 23. SAMHD1 can degrade HIV-1 RNA in the absence of reverse transcription.

To exclude the effect of the viral RT RNase H activity on the HIV-1 genomic RNA level, RNase H-defective HIV-1 (HIV-1_{D443N}) were used. The level of HIV-1_{D443N} RNA was lower in SAMHD1_{WT}-expressing cells compared with mock-transfected cells. (* indicates significant differences compared with the mock-transfected control at $P < 0.05$ using the two-tailed Student's t test).

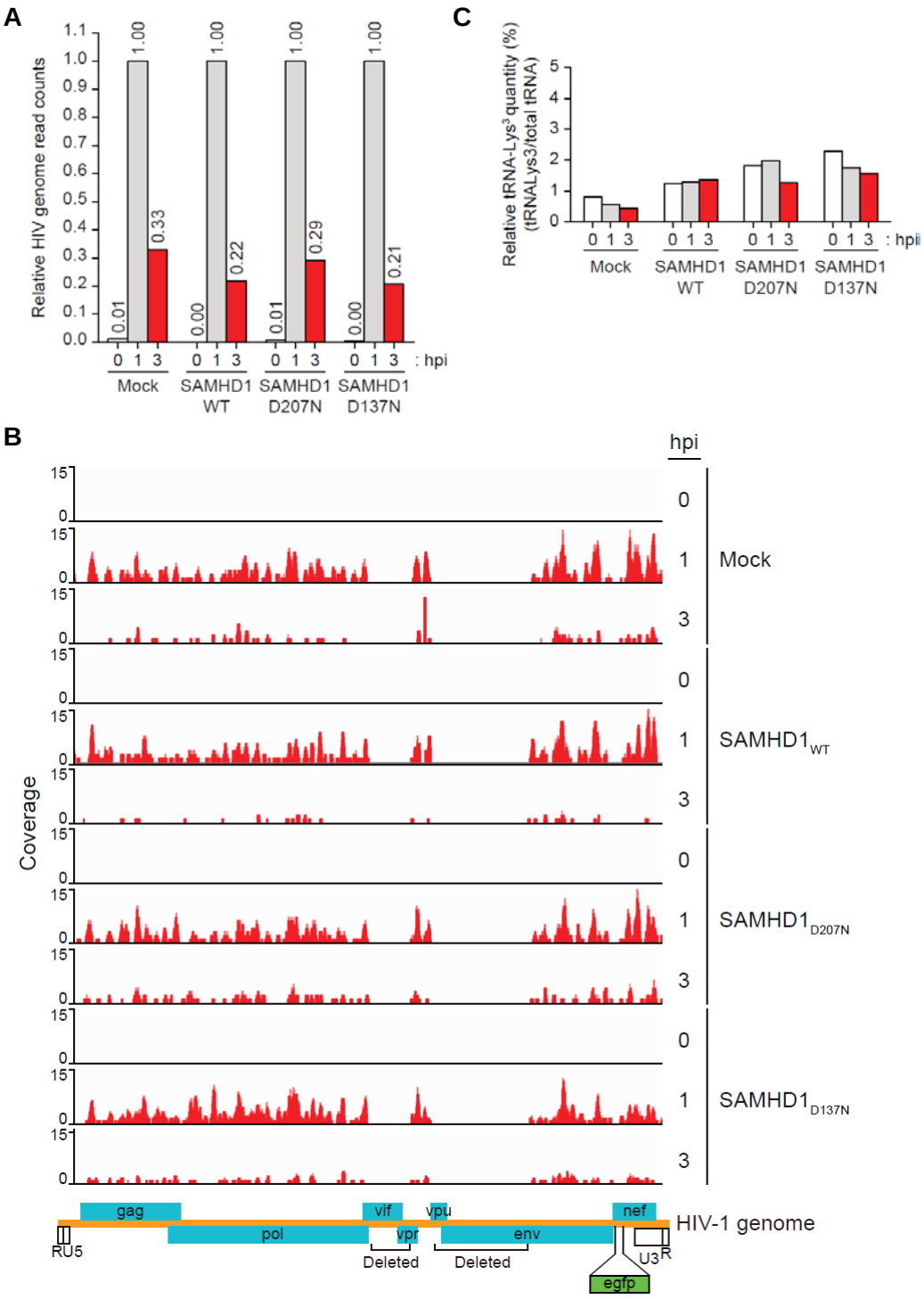
A
Relative HIV genome read counts
1.1
1.0
0.9
0.8
0.7
0.6
0.5
0.4
0.3
0.2
0.1
0.0
1.00
1.00
1.00
1.00
0.01
0.33
0.00
0.22
0.01
0.29
0.00
0.21
0 1 3
: hpi
Mock
SAMHD1 WT
SAMHD1 D207N
SAMHD1 D137N
C
Relative tRNA-Lys3 quantity (%)
(tRNALys3/total tRNA)
5
4
3
2
1
0
0 1 3
: hpi
Mock
SAMHD1 WT
SAMHD1 D207N
SAMHD1 D137N
B
hpi
Coverage
15
0
0
1
3
Mock
SAMHD1WT
SAMHD1D207N
SAMHD1D137N
gag
pol
vif
vpr
vpu
env
nef
RU5
Deleted
Deleted
U3R
egfp
HIV-1 genome

Figure 24. RNA-Seq analysis of HIV-1 degradation by SAMHD1 after infection.

(A) Relative HIV-1 genome abundance in reads per kilobase per million mapped reads (RPKM) calculated from RNA-Seq data. **(B)** Coverage of the RNA-Seq data across the HIV-1 genome in U937 cells expressing $SAMHD1_{WT}$, $SAMHD1_{D207N}$ and $SAMHD1_{D137N}$ after HIV-1-GFP infection. A schematic diagram of the viral gene loci in the HIV-1 genome is shown below the coverage plots. **(C)** Relative quantity of $tRNA^{Lys3}$ based on the reads that mapped non-redundantly to the $tRNA^{Lys3}$ loci, expressed as percentiles of the total tRNAs mapped. Data are representative of two independent experiments.

mediated knockdown of SAMHD1 or Vpx-mediated degradation of endogenous SAMHD1 in THP-1 cells also caused an approximately four-fold increase in the HIV-1 genomic RNA level (Figure 25). To verify that SAMHD1 targets HIV-1 genomic RNA for degradation, I used RNA immunoprecipitation (RIP) assays (62) to test whether SAMHD1 associated with HIV-1 genomic RNA during infection. A significant enrichment of HIV-1 RNA was observed in the immunoprecipitates from cells expressing $SAMHD1_{WT}$-HA. The HIV-1 RNA enrichment was more pronounced for the $SAMHD1_{D207N}$-HA catalytic mutant with an approximately eight-fold increase (Figure 26), suggesting that SAMHD1 associates with HIV-1 genomic RNA. In contrast, interaction of $SAMHD1_{Q548A}$-HA with HIV-1 RNA was markedly reduced when compared with the $SAMHD1_{WT}$-HA, supporting that impaired binding of $SAMHD1_{Q548A}$-HA to HIV-1 RNA accounts for its inability to cleave short ssRNA and HIV-1 RNA (Figure 15).

Next, I analyzed the role of SAMHD1 RNase in regulating HIV-1 RNA stability in primary human monocyte-derived macrophages (MDMs) and $CD4^+$ T cells. Cell surface expression of MDM-differentiation markers (CD71, CD80, and CD86) was increased 3 days after treatment with M-CSF and GM-CSF (Figure 27). The activation state of $CD4^+$ T cells was analyzed by monitoring the surface expression of the activation markers CD25 and CD69 at days 0, 3,

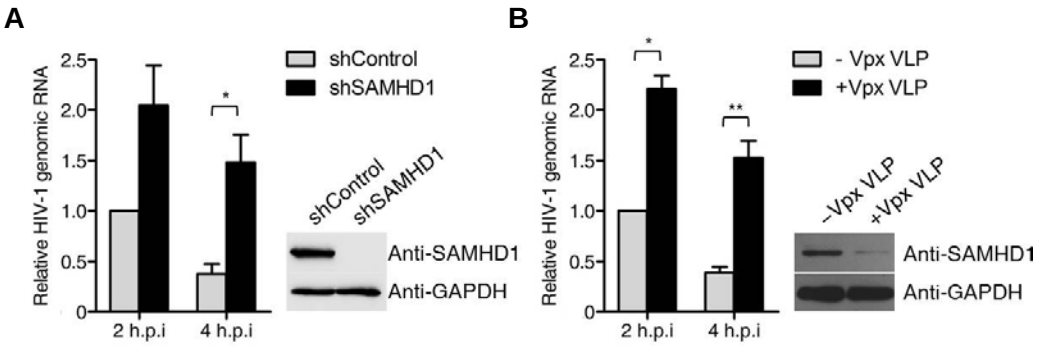
A
B
Relative HIV-1 genomic RNA
2.5
2.0
1.5
1.0
0.5
0
2 h.p.i
4 h.p.i
*
shControl
shSAMHD1
shControl
shSAMHD1
Anti-SAMHD1
Anti-GAPDH
- Vpx VLP
+Vpx VLP
**
-Vpx VLP
+Vpx VLP

Figure 25. HIV-1 RNA was stabilized when SAMHD1 was depleted.

shRNA-mediated silencing of SAMHD1 **(A)** or Vpx-mediated degradation of SAMHD1 **(B)** in THP-1 cells increases HIV-1 RNA stability. THP-1 cells expressing shRNAs, Vpx or negative control were treated with PMA for 24 h followed by infection with HIV-1-GFP. The total viral RNA was quantified by qRT-PCR at the indicated times post-infection. Knockdown efficiency was determined by immunoblot analysis. (* and ** indicate significant differences compared with shControl or –Vpx VLP control at $P < 0.05$ and $P < 0.001$, respectively, using the two-tailed Student's t test).

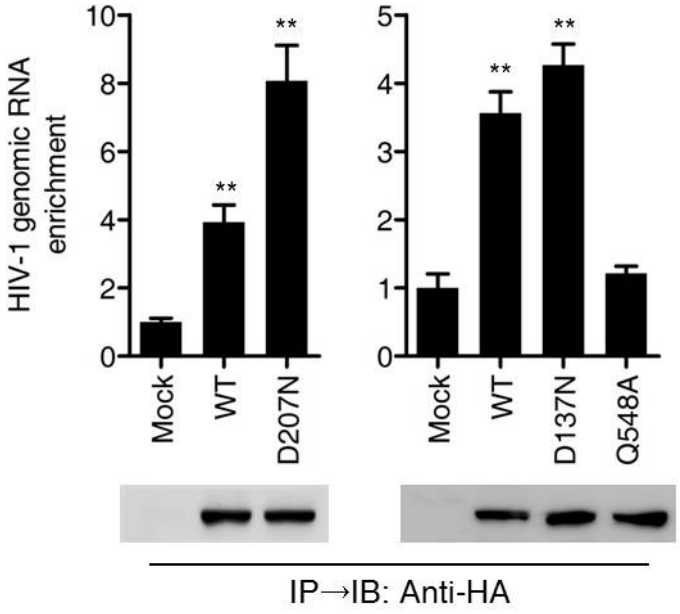
HIV-1 genomic RNA enrichment
10
8
6
4
2
0
**
**
Mock
WT
D207N
5
4
3
2
1
0
**
**
Mock
WT
D137N
Q548A
IP→IB: Anti-HA

Figure 26. Enrichment of HIV-1 genomic RNA in the SAMHD1 immunoprecipitates.

U937 cells containing the empty vector (mock) and vectors encoding $SAMHD1_{WT}$-HA, $SAMHD1_{D207N}$-HA, or $SAMHD1_{Q548A}$-HA were infected for 90 min with HIV-1-GFP. SAMHD1 was immunoprecipitated using anti-HA antibodies. The purified RNAs in the immunoprecipitates were quantified by qRT-PCR using HIV-1 *gag*-specific primers. (** indicates significant differences compared with the mock-transfected control at $P < 0.001$ using the two-tailed Student's t test).

A

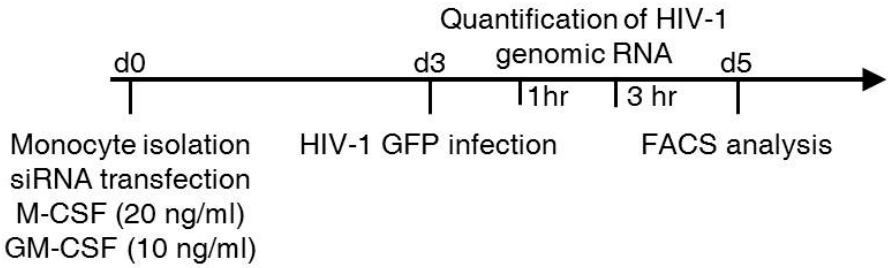
Quantification of HIV-1
genomic RNA
d0
d3
1hr
3 hr
d5
Monocyte isolation
siRNA transfection
M-CSF (20 ng/ml)
GM-CSF (10 ng/ml)
HIV-1 GFP infection
FACS analysis

B

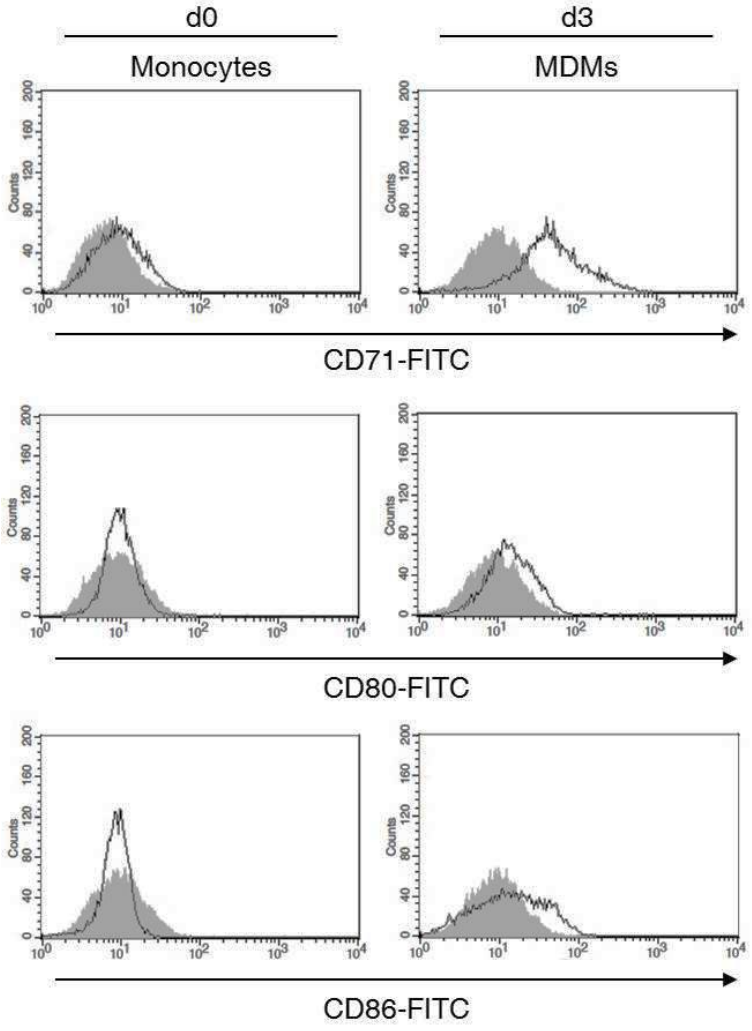
d0
d3
Monocytes
MDMs
Counts
CD71-FITC
CD80-FITC
CD86-FITC

Figure 27. Differentiation of monocytes into MDMs.

The experimental design for time course analysis is shown. $CD14^+$ monocytes derived from three donors were treated with M-CSF and GM-CSF and differentiated to MDMs for 3 days. The differentiation state of monocytes was analyzed by monitoring the surface expression of the markers (CD71, CD80, and CD86) by flow cytometry.

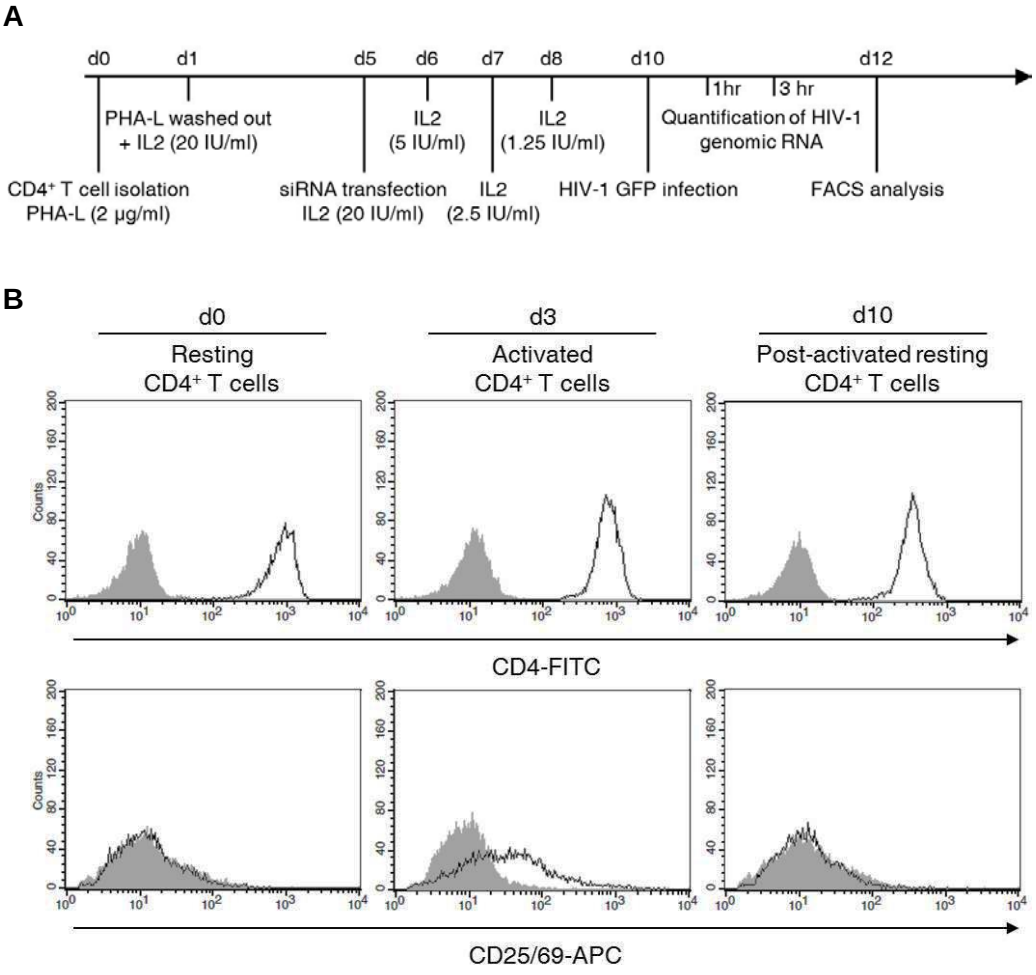
A
d0
d1
d5
d6
d7
d8
d10
d12
1hr
3 hr
PHA-L washed out
+ IL2 (20 IU/ml)
IL2
(5 IU/ml)
IL2
(1.25 IU/ml)
Quantification of HIV-1
genomic RNA
CD4+ T cell isolation
PHA-L (2 µg/ml)
siRNA transfection
IL2 (20 IU/ml)
IL2
(2.5 IU/ml)
HIV-1 GFP infection
FACS analysis
B
d0
Resting
CD4+ T cells
d3
Activated
CD4+ T cells
d10
Post-activated resting
CD4+ T cells
Counts
CD4-FITC
CD25/69-APC

Figure 28. Activation of $CD4^+$ T cells.

The experimental design for time course analysis is shown. The PBMC-derived $CD4^+$ T cells from three donors were activated, and post-activation resting $CD4^+$ T cells were obtained as previously described. Expression of CD4 was analyzed by flow cytometry using FITC-conjugated anti-CD4 antibody. The activation state of $CD4^+$ T cells was analyzed by monitoring the surface expression of the activation markers CD25 and CD69.

and 10 (Figure 28). *SAMHD1* silencing in MDMs markedly reduced the cellular SAMHD1 levels (Figure 29A) and rendered MDMs more permissive to HIV-1 infection (Figure 29B and 31A), a result that is correlated with the increased stability of HIV-1 RNA. The enhancement of HIV-1 RNA stability ranged from approximately two to four-fold, depending on the donor (Figure 29). Similar to the results obtained using MDMs, *SAMHD1* silencing in resting $CD4^+$ T cells increased the infectivity of HIV-1 (Figure 30B and 31B). In these cells, increased HIV-1 RNA stability was observed 3 h.p.i (Figure 30C). The degradation of SAMHD1 by Vpx could also stabilize the viral RNAs of HIV-1 and HIV-1_{D443N} in resting $CD4^+$ T cells (Figure 32). These results show that similar to the U937 monocytic cells, the antiviral activity of SAMHD1 is correlated with its RNase activity in primary human MDMs and resting $CD4^+$ T cells. Biochemical fractionation revealed that SAMHD1 is localized in both the cytoplasm and nucleus of MDMs and monocytes (Figure 33), which is consistent with previous observations (6, 34). Considering that cytoplasmic SAMHD1 can block HIV-1 infection (69, 70), these data suggest that after virus uncoating, SAMHD1 associates with and degrades HIV-1 RNA in the cytoplasm, thereby restricting HIV-1 replication.

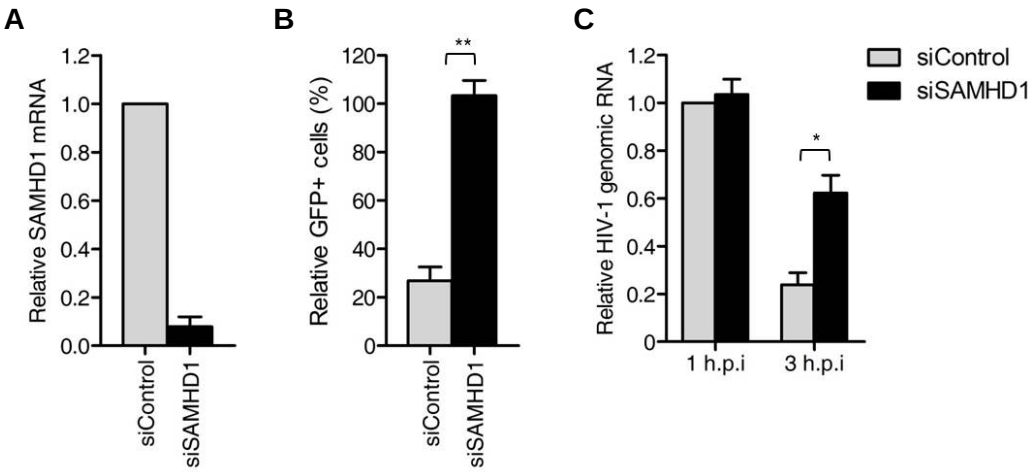
A
Relative SAMHD1 mRNA
1.2
1.0
0.8
0.6
0.4
0.2
0.0
siControl
siSAMHD1
B
Relative GFP+ cells (%)
120
100
80
60
40
20
0
**
siControl
siSAMHD1
C
Relative HIV-1 genomic RNA
1.2
1.0
0.8
0.6
0.4
0.2
0
*
1 h.p.i
3 h.p.i
siControl
siSAMHD1

Figure 29. SAMHD1 degrades HIV-1 genomic RNA in primary human MDMs.

$CD14^+$ monocytes isolated from three donors were differentiated into MDMs. MDMs were transfected with siRNA to *SAMHD1* or control siRNA and then infected with 100 ng of HIV-1-GFP. **(A)** The efficiency of *SAMHD1* knockdown was evaluated by qRT-PCR. **(B)** Quantification of GFP-positive cells by flow cytometry of MDMs. **(C)** Total viral RNA was quantified at the indicated times post-infection by qRT-PCR using *gfp*-specific primers. The data were normalized to an internal control gene (β-actin). (* and ** indicate significant differences compared with siControl at $P < 0.05$ and $P < 0.001$, respectively, using the two-tailed Student's t test).

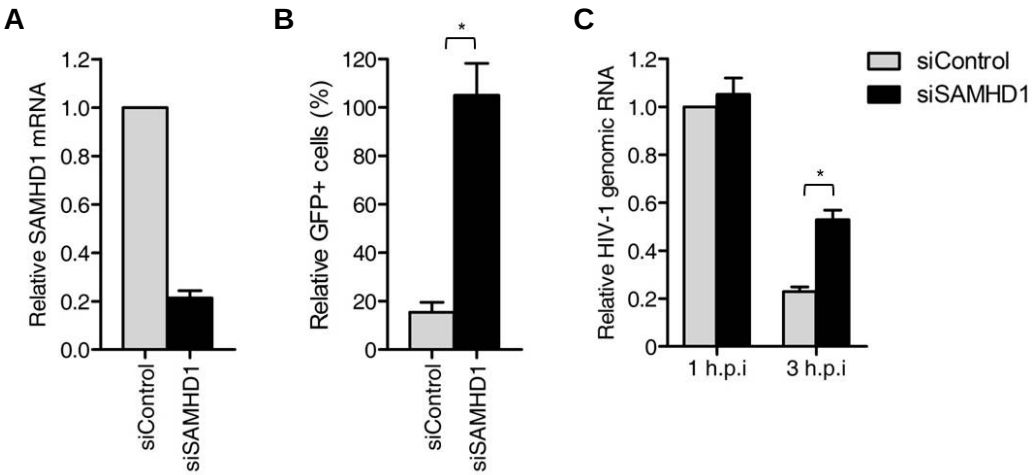
A
Relative SAMHD1 mRNA
1.2
1.0
0.8
0.6
0.4
0.2
0.0
siControl
siSAMHD1
B
Relative GFP+ cells (%)
120
100
80
60
40
20
0
*
siControl
siSAMHD1
C
Relative HIV-1 genomic RNA
1.2
1.0
0.8
0.6
0.4
0.2
0
*
1 h.p.i
3 h.p.i
siControl
siSAMHD1

Figure 30. SAMHD1 degrades HIV-1 genomic RNA in primary human CD4$^+$ T cells.

Post-activated resting CD4$^+$ T cells from three donors were transfected with siRNA to *SAMHD1* or control siRNA and then infected with 100 ng of HIV-1-GFP. **(A)** The efficiency of *SAMHD1* knockdown was evaluated by qRT-PCR. **(B)** Quantification of GFP-positive cells by flow cytometry of MDMs. **(C)** Total viral RNA was quantified at the indicated times post-infection by qRT-PCR using *gfp*-specific primers. The data were normalized to an internal control gene (β-actin). (* indicates significant differences compared with siControl at $P < 0.05$ using the two-tailed Student's t test).

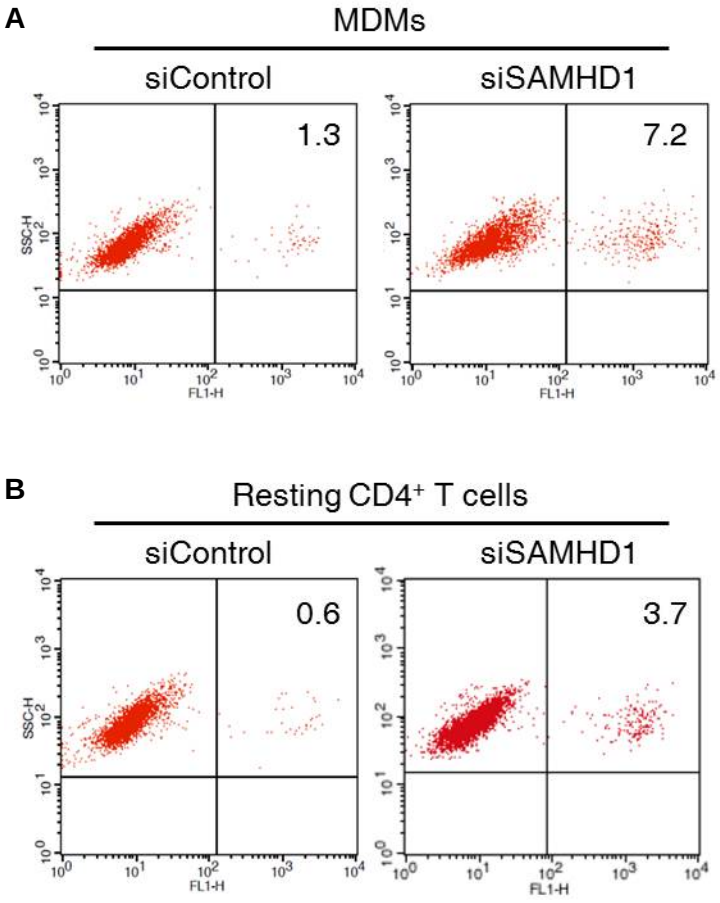
A
MDMs
siControl
siSAMHD1
1.3
7.2
SSC-H
FL1-H
B
Resting CD4+ T cells
siControl
siSAMHD1
0.6
3.7
SSC-H
FL1-H

Figure 31. Knockdown of SAMHD1 in MDMs and resting CD4$^+$ T cells increases HIV-1-GFP infectivity.

MDMs **(A)** and CD4$^+$ T cells **(B)** were transfected with siRNA to *SAMHD1* or control siRNA and then 100 ng of HIV-1-GFP. Flow cytometric analysis 48 h.p.i to measure the percentage of GFP-positive cells.

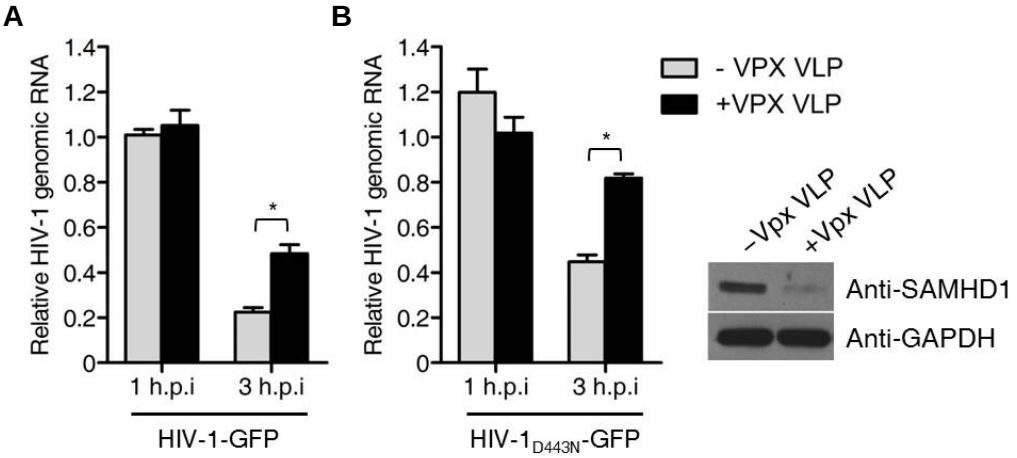
A
B
Relative HIV-1 genomic RNA
1.4
1.2
1.0
0.8
0.6
0.4
0.2
0
1 h.p.i
3 h.p.i
*
HIV-1-GFP
HIV-1D443N-GFP
- VPX VLP
+VPX VLP
-Vpx VLP
+Vpx VLP
Anti-SAMHD1
Anti-GAPDH

Figure 32. Effect of Vpx treatment on the HIV-1 RNA stability in resting $CD4^+$ T cells.

Resting $CD4^+$ T cells were challenged with HIV-1-GFP **(A)** or HIV-1-GFP_{D443N} **(B)** in the presence of Vpx VLP. Total viral RNA was quantified at the indicated times post-infection by qRT-PCR using *gfp*-specific primers. The data were normalized to an internal control gene (β-actin). Knockdown efficiency was determined by immunoblot analysis. (* indicates significant differences compared with – Vpx control at $P < 0.05$ using the two-tailed Student's t test).

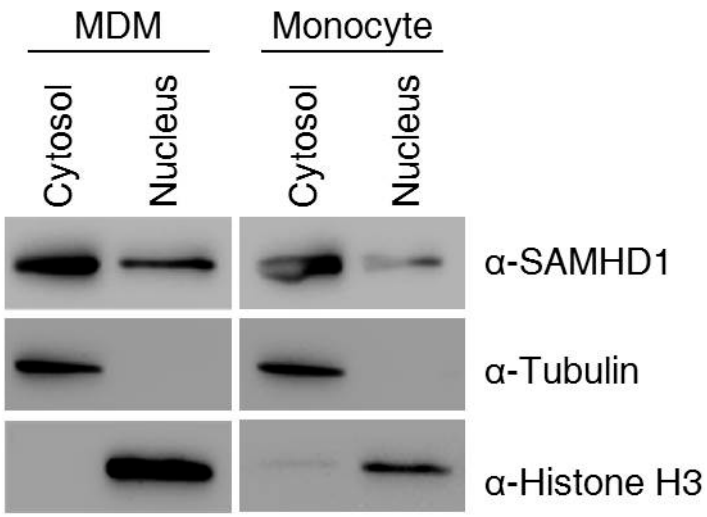
MDM
Monocyte
Cytosol
Nucleus
Cytosol
Nucleus
α-SAMHD1
α-Tubulin
α-Histone H3

Figure 33. Cellular distribution of SAMHD1 in both the cytoplasm and nucleus.

Nuclear and cytoplasmic fractions were prepared from MDMs or monocytes and analyzed by immunoblotting with anti-SAMHD1 antibody. Tubulin and Histone H3 served as cytoplasmic and nuclear markers, respectively.

5. Phosphorylation of SAMHD1 regulates RNase activity.

The phosphorylation of SAMHD1 at T592 causes the loss of HIV-1 restriction without decreasing cellular dNTP levels (32, 33, 64). I tested whether the phosphorylation of SAMHD1 affects its RNase activity in HIV-1 restriction. In PMA-treated U937 cells where $SAMHD1_{WT}$ is not phosphorylated on residue T592 (32, 33), $SAMHD1_{WT}$ blocked HIV-1 infection. In contrast, $SAMHD1_{T592D}$ containing the phosphomimetic D residue was unable to inhibit HIV-1 infection (Figure 34), confirming previous results (32). Notably, the stability of HIV-1 genomic RNA was enhanced by three to four-fold in cells expressing $SAMHD1_{T592D}$ compared with cells expressing $SAMHD1_{WT}$ (Figure 35). In contrast to this *in vivo* observation, the recombinant $SAMHD1_{T592D}$ protein was as effective as the $SAMHD1_{WT}$ and the nonphosphorable $SAMHD1_{T592V}$ in degrading ssRNA substrates *in vitro* (Figure 36). Phosphorylation did not appears to influence the structural conformation (19), oligomerization and dNTPase activity (32), or *in vitro* RNase activity of the enzyme. RIP analysis revealed that $SAMHD1_{WT}$ and $SAMHD1_{T592D}$ bound to HIV-1 genomic RNA with similar affinities, indicating that phosphorylation of SAMHD1 T592 does not interfere with substrate binding (Figure 37). Therefore, the discrepancy between the *in vivo* and *in vitro* RNase activities suggests that

the phosphorylation of SAMHD1 might promote the recruitment of cellular factors that negatively regulate its RNase activity *in vivo*. Alternatively, SAMHD1 phosphorylation might interfere with the interaction of SAMHD1 with unidentified cofactors. My results reveal that the phosphorylation of SAMHD1 at T592 is a mechanism that negatively regulates its RNase activity and impedes HIV-1 restriction.

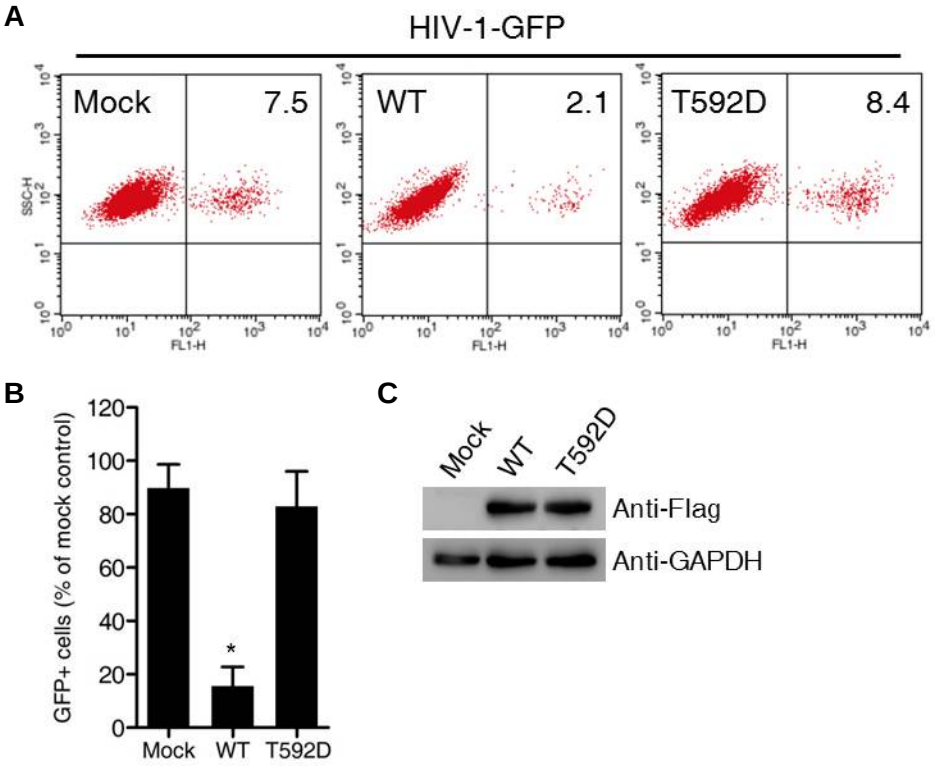
A
HIV-1-GFP
Mock
7.5
WT
2.1
T592D
8.4
SSC-H
FL1-H
B
GFP+ cells (% of mock control)
120
100
80
60
40
20
0
*
Mock
WT
T592D
C
Mock
WT
T592D
Anti-Flag
Anti-GAPDH

Figure 34. The role of SAMHD1 in the regulation of HIV-1 restriction by phosphorylation T592.

U937 cells stably expressing an empty vector (mock) or Flag-tagged SAMHD1 variants were treated with PMA and infected with 100 ng of pLaiΔenvGFP3. **(A)** Flow cytometric analysis 48 h.p.i to measure the percentage of GFP-positive cells. **(B)** The percentage of GFP-positive cells was calculated relative to the number of GFP-positive mock-transfected cells. **(C)** Immunoblot analysis of cell extracts using the anti–Flag antibody. GAPDH was used as a loading control.

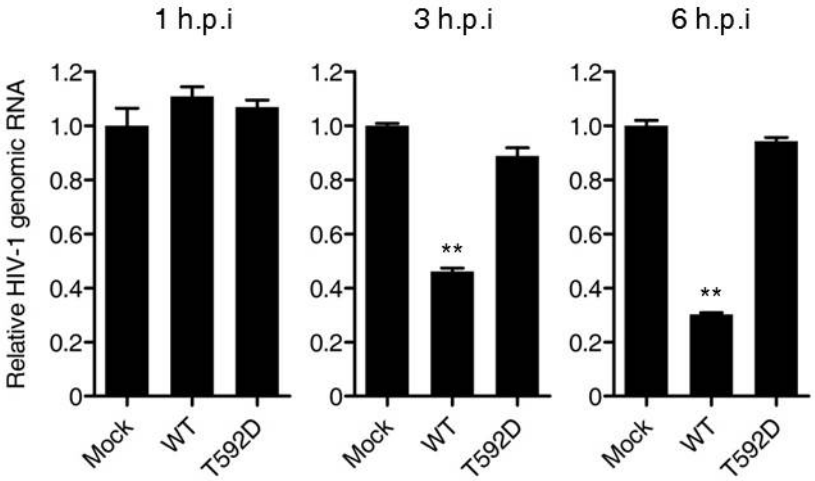
1 h.p.i
3 h.p.i
6 h.p.i
Relative HIV-1 genomic RNA
1.2
1.0
0.8
0.6
0.4
0.2
0
**
**
Mock
WT
T592D

Figure 35. SAMHD1 phosphorylated on residue T592 is unable to degrade HIV-1 RNA.

U937 cells stably expressing an empty vector (mock), Flag-tagged $SAMHD1_{WT}$ or $SAMHD1_{T592D}$ were treated with PMA and infected with 100 ng of HIV-1-GFP. The HIV-1 RNA content was quantified by qRT-PCR using HIV-1 *gag*-specific primers. The data were normalized to an internal β-actin. (** indicates significant differences compared with the mock-transfected control at $P < 0.001$ using the two-tailed Student's t test).

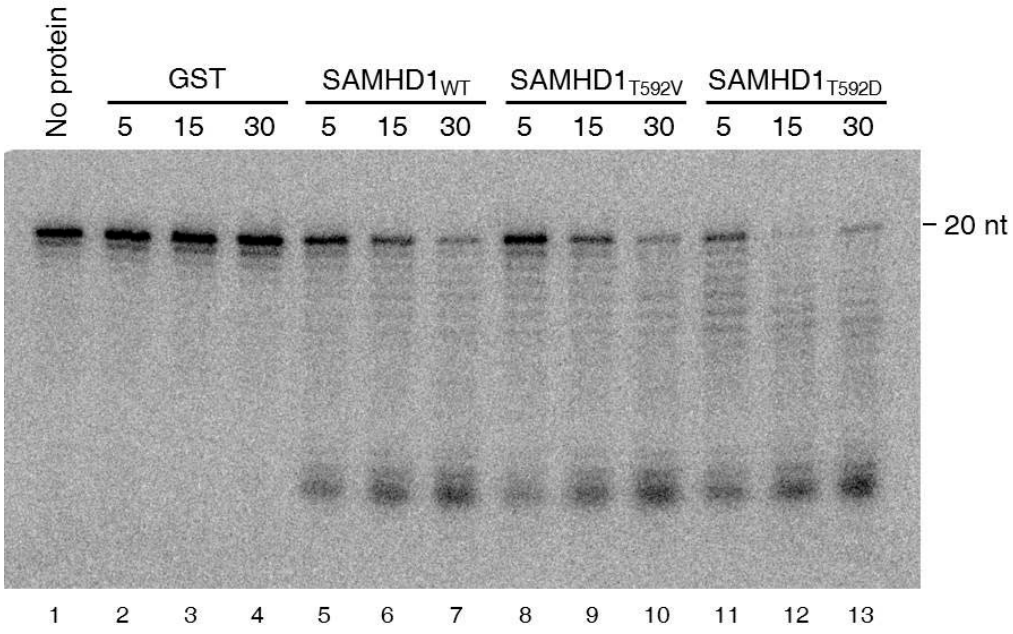
No protein
GST
SAMHD1WT
SAMHD1T592V
SAMHD1T592D
5 15 30 5 15 30 5 15 30 5 15 30
20 nt
1 2 3 4 5 6 7 8 9 10 11 12 13

Figure 36. The RNase activity of SAMHD1$_{T592D}$ is not affected.

Recombinant SAMHD1$_{T592V}$ and SAMHD1$_{T592D}$ proteins were purified from *E. coli*. Purified proteins were incubated for 30 min at 37°C with various synthetic nucleic acid substrates (20-mers) that were 5'-end labeled with [γ-^{32}P]ATP. The products were analyzed by electrophoresis and autoradiography.

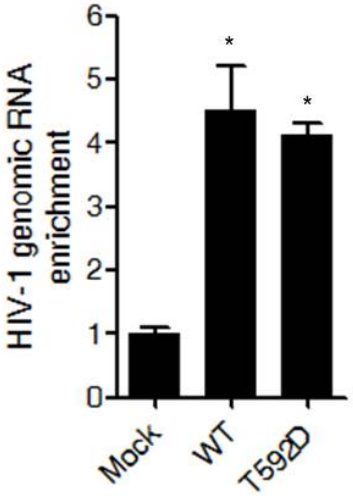
HIV-1 genomic RNA enrichment
6
5
4
3
2
1
0
*
*
Mock
WT
T592D

Figure 37. Effect of SAMHD1 T592 phosphorylation on substrate binding.

U937 cells expressing vector alone, $SAMHD1_{WT}$ or $SAMHD1_{T592D}$ were infected for 90 min with HIV-1-GFP and crosslinked by formaldehyde. Cell lysates were immunoprecipitated with anti-Flag antibody. Purified RNAs from the immunoprecipitates were quantified by qRT-PCR using HIV-1 *gag*-specific primer.

DISCUSSION

I identify SAMHD1 as a phospho-regulated RNase that blocks HIV-1 infection through a direct cleavage of HIV-1 genomic RNA. Several observations are consistent with the model that SAMHD1-mediated HIV-1 restriction occurs through the action of the RNase but not the dNTPase activity of SAMHD1 (Figure 38). First, the dNTPase-negative and RNase-positive $SAMHD1_{D137N}$ mutant is able to block HIV-1 replication, whereas the dNTPase-positive and RNase-negative $SAMHD1_{Q548A}$ mutant with a phenotype opposite to the $SAMHD1_{D137N}$ mutant is defective in restricting HIV-1 infection. Second, the phosphorylation of SAMHD1 modulates the ability of this enzyme to restrict HIV-1 infection but does not affect its ability to alter cellular dNTP levels (32, 33, 64), and the RNase function of SAMHD1 in HIV-1 restriction is regulated by phosphorylation. Third, the role of dNTPase activity in HIV-1 restriction was consistent with the observation that exogenous deoxynucleosides (dNs; precursors of dNTPs) can alleviate SAMHD1-mediated restriction (28). However, in macrophages and resting $CD4^+$ T cells with low dNTP levels (71), the Vpx-mediated degradation of SAMHD1 is significantly more effective than the addition of exogenous dNs in overcoming HIV-1 restriction (6, 28), suggesting that an unknown function is involved in restriction.

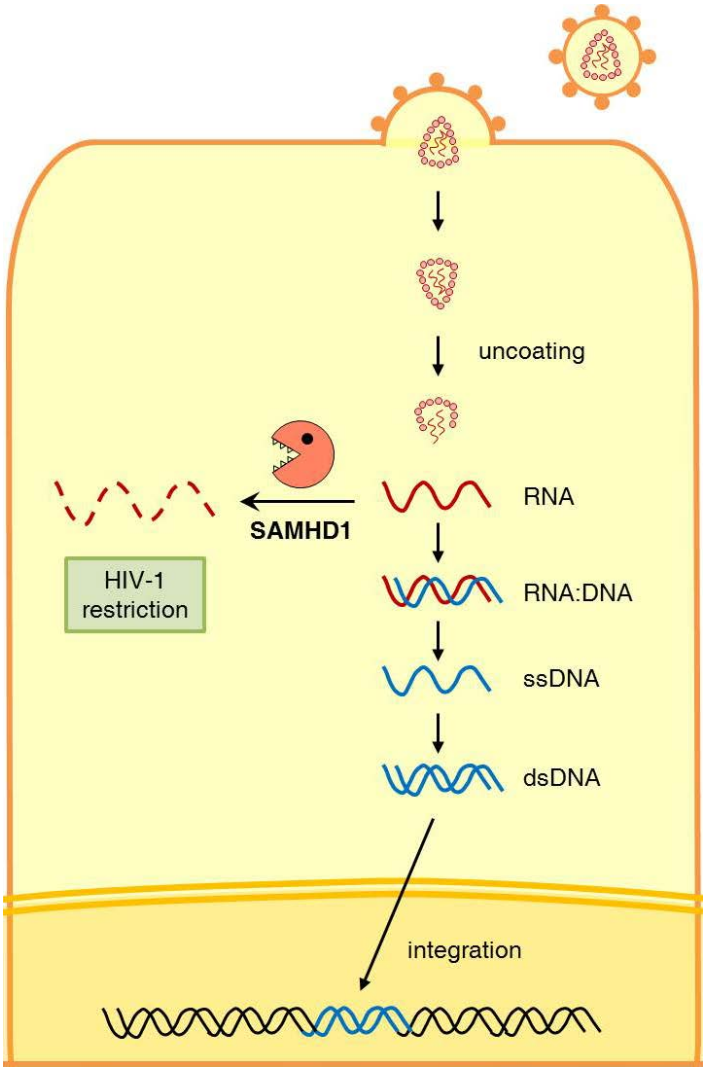

Figure 38. HIV-1 restriction mechanism of SAMHD1.

Once HIV-1 genomic RNA is released from the core in the cytoplasm, SAMHD1 recognizes and directly degrades the HIV-1 genomic RNA, therefore is able to block HIV-1 reverse transcription step.

The partial alleviation of SAMHD1-mediated HIV-1 restriction by the addition of exogenous dNs might be an indirect consequence of impaired RNA substrate binding and/or RNase activity of SAMHD1 caused by the increase in dGTP levels. The crystal structure of SAMHD1 catalytic core (aa. 120-626) reveals that this protein is dimeric and indicates a structural basis for the allosteric activation of catalytic activity against dNTPs by dGTP binding (18). In contrast, functional and structural analyses have demonstrated that SAMHD1 oligomerizes in a dGTP-dependent manner up to a tetramer and that the tetramerization of SAMHD1 is required for its dNTPase and anti-HIV-1 activities (19, 20). Notably, Yan et al. (20) observed that SAMHD1 with a mutation at the allosteric dGTP-binding site D137 did not undergo oligomerization and was mostly monomeric in the presence of dGTP. The mutation at D137 ($SAMHD1_{D137N}$) abolishes SAMHD1 dNTPase but not RNase activity (Figure 14), indicating that unlike the dNTPase activity, the tetramerization of SAMHD1 is not necessary for its RNase activity. Based on previous data as well as the results of my research, I propose that SAMHD1 is a dual-function enzyme exhibiting several mutually exclusive and predominant activities that depend on the dGTP pool, which is normally the smallest component of the total dNTP pool and is most affected by SAMHD1 knockdown (72). At low dGTP levels, SAMHD1 exists as monomers or dimers

that harbor active RNase but not dNTPase activity, enabling HIV-1 restriction through the cleavage of HIV-1 RNA. At high dGTP levels, SAMHD1 tetramerizes, yielding an enzyme with an inactive RNase but active dNTPase function, although there is no direct evidence for the correlation of dGTP-induced SAMHD1 tetramerization and the inactivation of RNase catalytic activity *in vivo* (Figure 39). An alternative but not mutually exclusive possibility is that the ssRNA and dNTP substrates might compete with each other for a common active site on the enzyme. Notably, dGTP is both a substrate and an activator of the SAMHD1 dNTPase function (18, 29). This model is consistent with several observations from previous studies: high levels of dGTP impair the binding of SAMHD1 to nucleic acid substrates *in vitro* (21, 32), the switch from a processive to distributive mode of ssRNA degradation in a dGTP-dependent manner (Figure 16) is indicative of competitive inhibition of ssRNA-binding by dGTP, and that the mutations in the D207 and D311 amino acids at the enzymatic catalytic site abolish both RNase and dNTPase activities (Figure 14). These two hypotheses may provide an explanation for why SAMHD1 blocks HIV-1 infection only in non-cycling cells with low dNTP levels, such as DCs and macrophages (4), but not in cycling cells with high dNTP levels (6, 32, 73). Another explanation might be that dNTP limitation in non-cycling cells, would slow down reverse transcription, and this could allow a sufficient time window

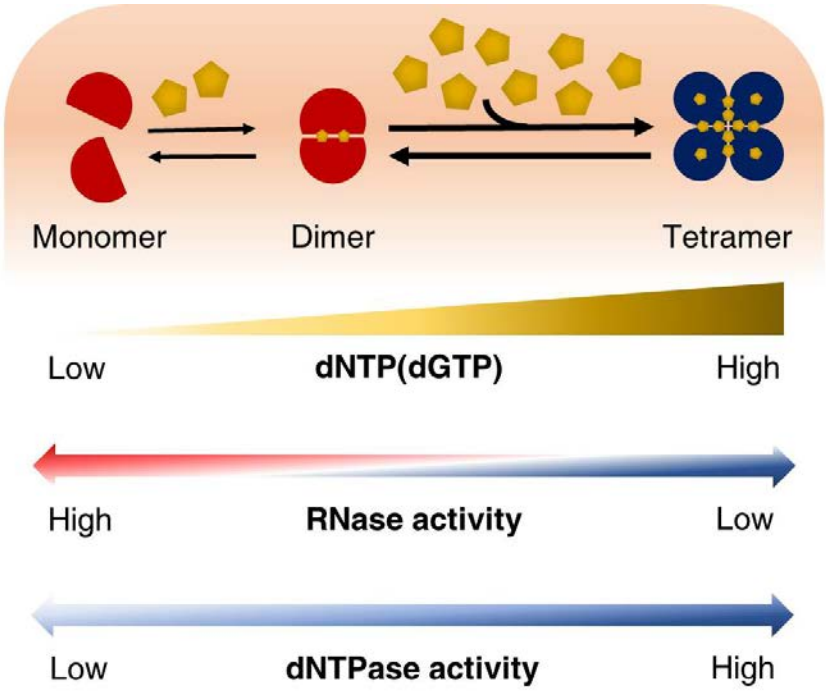

Figure 39. Regulation model of SAMHD1-dual enzymatic activities.

Tetramerization of SAMHD1 is required for its dNTPase activity in a dGTP-dependent manner. Conversely, the RNase activity of SAMHD1 does not depend on either dGTP binding or tetramer formation. It is possible that that tetramerization impairs RNase activity.

for the action of SAMHD1 RNase against HIV-1 RNA. Considering that uncontrolled and high dNTP concentrations are mutagenic for genome replication (74) and that dNTP destruction by SAMHD1 contributes to control of the dNTP concentration in proliferating cells (72), SAMHD1 dNTPase most likely has a more general role in regulating the dNTP pool by 'positive regulation' in which the accumulated dGTPs activate the SAMHD1 dNTPase activity, thereby preventing the overproduction of dNTPs.

It is unknown whether the anti-viral activity of SAMHD1 is specific to retroviruses, although SAMHD1 is known to restrict the infections caused by a diverse range of retroviruses (7, 8). Furthermore, it is unclear how retroviral RNAs are selectively targeted for degradation over various cellular RNAs. SAMHD1 RNase activity exhibits no apparent sequence specificity (Figure 7, 9 and 10). Exoribonucleases like SAMHD1 digest a diverse range of substrates from poly(A) to highly structured RNAs such as tRNA and rRNA. In some cases, exoribonuclease can act alone to process the substrate, but in most cases, a helicase or other cofactor is required to direct the RNA into the active site of the enzyme (75).

I can speculate that SAMHD1 specifically recognizes retroviral RNA-associated structural elements unique to retroviruses, such as RT or the tertiary structure of LTR. The absence of such retroviral determinants might

render cellular RNAs insensitive to SAMHD1. A variety of *cis*-elements or *trans*-acting regulatory factors, such as RNA-binding proteins, protect cellular RNAs from eukaryotic RNases (76). Therefore, the absence of these regulatory factors in retroviral genomes might result in the specific susceptibility of viral RNAs to degradation by SAMHD1.

Similar to mutations in *SAMHD1*, mutations in the genes encoding TREX1 and RNASEH2 cause AGS (44, 45). The exonuclease TREX1 digests excess cytosolic HIV-1 DNA that would otherwise trigger an innate immune response (54), and the endonuclease RNASEH2 degrades the RNA moiety of RNA:DNA hybrids (45, 46). The identification of SAMHD1 as an RNase suggests that similar to TREX1 and RNASEH2, SAMHD1 has a critical role in nucleic acid metabolism related to the prevention of an innate immune response; therefore, my results provide an insight into the mechanisms underlying HIV-1 restriction and the pathogenesis of AGS.

Based on my data and the links between the accumulation of nucleic acids and the inappropriate triggering of innate immune responses (36), the natural function of SAMHD1 is likely to clean up dysfunctional cellular RNAs or RNA species derived from endogenous retroelement, thus preventing an unwanted inflammatory response (Figure 40). Human endogenous retroviruses make up nearly 8% of the human genome and have been implicated in some

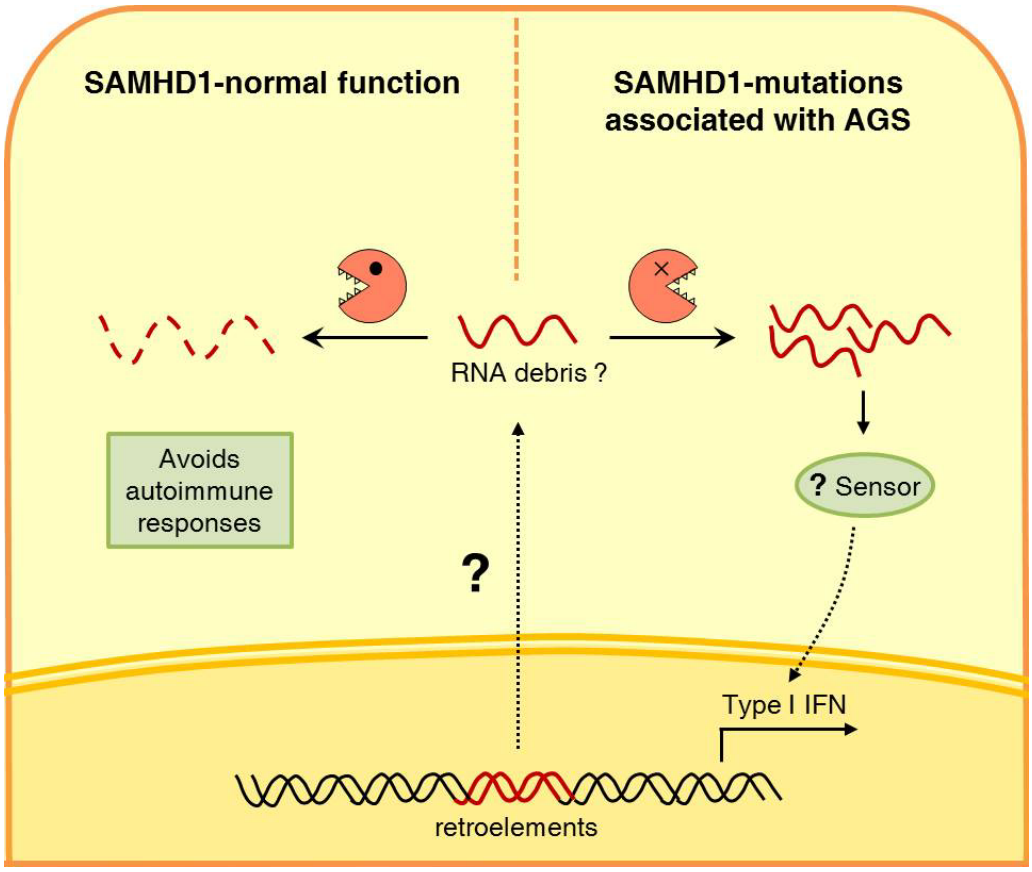

Figure 40. Model of AGS pathogenesis in deficiency of SAMHD1.

Lack of function mutations in SAMHD1 would impair the control of nucleic acid homeostasis. Accumulation RNA debris or RNA species derived from retroelements activats type I IFN pathway through unknown sensors. The aberrant activation of innate immune response could cause pro-inflammatory diseases such as AGS.

autoimmune diseases (77). In line with the specific recognition of HIV-1 RNA by SAMHD1 and the ability of SAMHD1 to restrict a wide range of retroviruses (7), the byproducts of human endogenous retroviruses are potentially major targets of SAMHD1. In addition, this mechanism may also explain the molecular basis of AGS and related lupus-like diseases in patients with loss-of-function mutations in SAMHD1 (14). The failure to degrade endogenous RNA debris is likely a principle pathway causing the aberrant activation of innate immune responses in individuals with SAMHD1-mediated autoimmune diseases. In fact, my observations reveal the direct association of SAMHD1 with RNA species in human cell lines. This unique property of SAMHD1 which affects the balance between HIV-1 infection and innate immune response could be exploited to develop a new class of intervention strategies for retroviruses and autoimmune diseases associated with nucleic acid metabolism.

REFERENCES

1. Geijtenbeek TB, DJ Krooshoop, DA Bleijs, SJ van Vliet, GC van Duijnhoven, V Grabovsky, R Alon, CG Figdor, and Y van Kooyk, DC-SIGN-ICAM-2 interaction mediates dendritic cell trafficking. Nat Immunol, 2000. 1(4): p. 353-7.

2. Lehner T, Y Wang, J Pido-Lopez, T Whittall, LA Bergmeier, and K Babaahmady, The emerging role of innate immunity in protection against HIV-1 infection. Vaccine, 2008. 26(24): p. 2997-3001.

3. Alter G, D Heckerman, A Schneidewind, L Fadda, CM Kadie, JM Carlson, C Oniangue-Ndza, M Martin, B Li, SI Khakoo, et al., HIV-1 adaptation to NK-cell-mediated immune pressure. Nature. 476(7358): p. 96-100.

4. Laguette N, B Sobhian, N Casartelli, M Ringeard, C Chable-Bessia, E Segeral, A Yatim, S Emiliani, O Schwartz, and M Benkirane, SAMHD1 is the dendritic- and myeloid-cell-specific HIV-1 restriction factor counteracted by Vpx. Nature, 2011. 474(7353): p. 654-7.

5. Hrecka K, C Hao, M Gierszewska, SK Swanson, M Kesik-Brodacka, S Srivastava, L Florens, MP Washburn, and J Skowronski, Vpx relieves inhibition of HIV-1 infection of macrophages mediated by the SAMHD1 protein. Nature, 2011. 474(7353): p. 658-61.

6. Baldauf HM, X Pan, E Erikson, S Schmidt, W Daddacha, M Burggraf, K Schenkova, I Ambiel, G Wabnitz, T Gramberg, et al., SAMHD1 restricts HIV-1 infection in resting CD4(+) T cells. Nat Med, 2012. 18: p. 1682-1689.

7. White TE, A Brandariz-Nunez, J Carlos Valle-Casuso, S Amie, L Nguyen, B Kim, J Brojatsch, and F Diaz-Griffero, Contribution of SAM and HD domains to retroviral restriction mediated by human SAMHD1. Virology, 2013. 436(1): p. 81-90.

8. Gramberg T, T Kahle, N Bloch, S Wittmann, E Mullers, W Daddacha, H Hofmann, B Kim, D Lindemann, and NR Landau, Restriction of diverse retroviruses by SAMHD1. Retrovirology, 2013. 10: p. 26.

9. Ueno F, H Shiota, M Miyaura, A Yoshida, A Sakurai, J Tatsuki, AH Koyama, H Akari, A Adachi, and M Fujita, Vpx and Vpr proteins of HIV-2 up-regulate the viral infectivity by a distinct mechanism in lymphocytic cells. Microbes Infect, 2003. 5(5): p. 387-95.

10. Fujita M, M Otsuka, M Miyoshi, B Khamsri, M Nomaguchi, and A Adachi, Vpx is critical for reverse transcription of the human immunodeficiency virus type 2 genome in macrophages. J Virol, 2008. 82(15): p. 7752-6.

11. Srivastava S, SK Swanson, N Manel, L Florens, MP Washburn, and J Skowronski, Lentiviral Vpx accessory factor targets VprBP/DCAF1 substrate adaptor for cullin 4 E3 ubiquitin ligase to enable macrophage infection. PLoS Pathog, 2008. 4(5): p. e1000059.

12. Bergamaschi A, D Ayinde, A David, E Le Rouzic, M Morel, G Collin, D Descamps, F Damond, F Brun-Vezinet, S Nisole, et al., The human immunodeficiency virus type 2 Vpx protein usurps the CUL4A-DDB1 DCAF1 ubiquitin ligase to overcome a postentry block in macrophage infection. J Virol, 2009. 83(10): p. 4854-60.

13. Li N, W Zhang, and X Cao, Identification of human homologue of mouse IFN-gamma induced protein from human dendritic cells. Immunol Lett, 2000. 74(3): p. 221-4.

14. Rice GI, J Bond, A Asipu, RL Brunette, IW Manfield, IM Carr, JC Fuller, RM Jackson, T Lamb, TA Briggs, et al., Mutations involved in Aicardi-Goutieres syndrome implicate SAMHD1 as regulator of the innate immune response. Nat Genet, 2009. 41(7): p. 829-32.

15. Liao W, Z Bao, C Cheng, YK Mok, and WS Wong, Dendritic cell-derived interferon-gamma-induced protein mediates tumor necrosis factor-alpha stimulation of human lung fibroblasts. Proteomics, 2008. 8(13): p. 2640-50.

16. Qiao F and JU Bowie, The many faces of SAM. Sci STKE, 2005. 2005(286): p. re7.

17. Aravind L and EV Koonin, The HD domain defines a new superfamily of metal-dependent phosphohydrolases. Trends Biochem Sci, 1998. 23(12): p. 469-72.

18. Goldstone DC, V Ennis-Adeniran, JJ Hedden, HC Groom, GI Rice, E Christodoulou, PA Walker, G Kelly, LF Haire, MW Yap, et al., HIV-1 restriction factor SAMHD1 is a deoxynucleoside triphosphate triphosphohydrolase. Nature, 2011. 480(7377): p. 379-82.

19. Ji X, Y Wu, J Yan, J Mehrens, H Yang, M DeLucia, C Hao, AM Gronenborn, J Skowronski, J Ahn, et al., Mechanism of allosteric activation of SAMHD1 by dGTP. Nat Struct Mol Biol, 2013. 20(11): p. 1304-9.

20. Yan J, S Kaur, M DeLucia, C Hao, J Mehrens, C Wang, M Golczak, K Palczewski, AM Gronenborn, J Ahn, et al., Tetramerization of SAMHD1 is required for biological activity and inhibition of HIV infection. J Biol Chem, 2013. 288(15): p. 10406-17.

21. Beloglazova N, R Flick, A Tchigvintsev, G Brown, A Popovic, B Nocek, and AF Yakunin, Nuclease Activity of the Human SAMHD1 Protein Implicated in the Aicardi-Goutieres Syndrome and HIV-1 Restriction. J Biol Chem, 2013. 288(12): p. 8101-10.

22. Brandariz-Nunez A, JC Valle-Casuso, TE White, N Laguette, M Benkirane, J Brojatsch, and F Diaz-Griffero, Role of SAMHD1 nuclear localization in restriction of HIV-1 and SIVmac. Retrovirology. 9: p. 49.

23. Hofmann H, EC Logue, N Bloch, W Daddacha, SB Polsky, ML Schultz, B Kim, and NR Landau, The Vpx lentiviral accessory protein targets SAMHD1 for degradation in the nucleus. J Virol. 86(23): p. 12552-60.

24. Amie SM, E Noble, and B Kim, Intracellular nucleotide levels and the control of retroviral infections. Virology. 436(2): p. 247-54.

25. Gao WY, A Cara, RC Gallo, and F Lori, Low levels of deoxynucleotides in peripheral blood lymphocytes: a strategy to inhibit human immunodeficiency virus type 1 replication. Proc Natl Acad Sci U S A, 1993. 90(19): p. 8925-8.

26. Diamond TL, M Roshal, VK Jamburuthugoda, HM Reynolds, AR Merriam, KY Lee, M Balakrishnan, RA Bambara, V Planelles, S Dewhurst, et al., Macrophage tropism of HIV-1 depends on efficient cellular dNTP utilization by reverse transcriptase. J Biol Chem, 2004. 279(49): p. 51545-53.

27. Zack JA, SJ Arrigo, SR Weitsman, AS Go, A Haislip, and IS Chen, HIV-1 entry into quiescent primary lymphocytes: molecular analysis reveals a labile, latent viral structure. Cell, 1990. 61(2): p. 213-22.

28. Lahouassa H, W Daddacha, H Hofmann, D Ayinde, EC Logue, L Dragin, N Bloch, C Maudet, M Bertrand, T Gramberg, et al., SAMHD1 restricts the replication of human immunodeficiency virus type 1 by depleting the intracellular pool of deoxynucleoside triphosphates. Nat Immunol, 2012. 13(3): p. 223-8.

29. Powell RD, PJ Holland, T Hollis, and FW Perrino, Aicardi-Goutieres syndrome gene and HIV-1 restriction factor SAMHD1 is a dGTP-regulated deoxynucleotide triphosphohydrolase. J Biol Chem, 2011. 286(51): p. 43596-600.

30. Kim B, LA Nguyen, W Daddacha, and JA Hollenbaugh, Tight interplay among SAMHD1 protein level, cellular dNTP levels, and HIV-1 proviral DNA synthesis

kinetics in human primary monocyte-derived macrophages. J Biol Chem. 287(26): p. 21570-4.

31. St Gelais C, S de Silva, SM Amie, CM Coleman, H Hoy, JA Hollenbaugh, B Kim, and L Wu, SAMHD1 restricts HIV-1 infection in dendritic cells (DCs) by dNTP depletion, but its expression in DCs and primary CD4+ T-lymphocytes cannot be upregulated by interferons. Retrovirology, 2012. 9: p. 105.

32. White TE, A Brandariz-Nunez, JC Valle-Casuso, S Amie, LA Nguyen, B Kim, M Tuzova, and F Diaz-Griffero, The Retroviral Restriction Ability of SAMHD1, but Not Its Deoxynucleotide Triphosphohydrolase Activity, Is Regulated by Phosphorylation. Cell Host Microbe, 2013. 13(4): p. 441-51.

33. Cribier A, B Descours, AL Valadao, N Laguette, and M Benkirane, Phosphorylation of SAMHD1 by Cyclin A2/CDK1 Regulates Its Restriction Activity toward HIV-1. Cell Rep, 2013. 3(4): p. 1036-43.

34. Goncalves A, E Karayel, GI Rice, KL Bennett, YJ Crow, G Superti-Furga, and T Burckstummer, SAMHD1 is a nucleic-acid binding protein that is mislocalized due to aicardi-goutieres syndrome-associated mutations. Hum Mutat, 2012. 33(7): p. 1116-22.

35. Tungler V, W Staroske, B Kind, M Dobrick, S Kretschmer, F Schmidt, C Krug, M Lorenz, O Chara, P Schwille, et al., Single-stranded nucleic acids promote SAMHD1 complex formation. J Mol Med (Berl), 2013.

36. Crow YJ and J Rehwinkel, Aicardi-Goutieres syndrome and related phenotypes: linking nucleic acid metabolism with autoimmunity. Hum Mol Genet, 2009. 18(R2): p. R130-6.

37. Stetson DB and R Medzhitov, Antiviral defense: interferons and beyond. J Exp Med, 2006. 203(8): p. 1837-41.

38. Crow MK, Type I interferon in systemic lupus erythematosus. Curr Top Microbiol Immunol, 2007. 316: p. 359-86.

39. Ronnblom L and V Pascual, The innate immune system in SLE: type I interferons and dendritic cells. Lupus, 2008. 17(5): p. 394-9.

40. Aicardi J and F Goutieres, Systemic lupus erythematosus or Aicardi-Goutieres syndrome? Neuropediatrics, 2000. 31(3): p. 113.

41. Dale RC, SP Tang, JZ Heckmatt, and FM Tatnall, Familial systemic lupus erythematosus and congenital infection-like syndrome. Neuropediatrics, 2000. 31(3): p. 155-8.

42. Ronnblom L and V Pascual, The innate immune system in SLE: type I interferons and dendritic cells. Lupus, 2008. 17(5): p. 394-399.

43. Rasmussen M, K Skullerud, SJ Bakke, P Lebon, and FL Jahnsen, Cerebral thrombotic microangiopathy and antiphospholipid antibodies in Aicardi-Goutieres syndrome report of two sisters. Neuropediatrics, 2005. 36(1): p. 40-44.

44. Crow YJ, BE Hayward, R Parmar, P Robins, A Leitch, M Ali, DN Black, H van Bokhoven, HG Brunner, BC Hamel, et al., Mutations in the gene encoding the 3'-5' DNA exonuclease TREX1 cause Aicardi-Goutieres syndrome at the AGS1 locus. Nat Genet, 2006. 38(8): p. 917-20.

45. Crow YJ, A Leitch, BE Hayward, A Garner, R Parmar, E Griffith, M Ali, C Semple, J Aicardi, R Babul-Hirji, et al., Mutations in genes encoding ribonuclease H2 subunits

cause Aicardi-Goutieres syndrome and mimic congenital viral brain infection. Nat Genet, 2006. 38(8): p. 910-6.

46. Perrino FW, S Harvey, NM Shaban, and T Hollis, RNaseH2 mutants that cause Aicardi-Goutieres syndrome are active nucleases. J Mol Med (Berl), 2009. 87(1): p. 25-30.

47. Rice GI, PR Kasher, GM Forte, NM Mannion, SM Greenwood, M Szynkiewicz, JE Dickerson, SS Bhaskar, M Zampini, TA Briggs, et al., Mutations in ADAR1 cause Aicardi-Goutieres syndrome associated with a type I interferon signature. Nat Genet. 44(11): p. 1243-8.

48. Rice GI, Y del Toro Duany, EM Jenkinson, GM Forte, BH Anderson, G Ariaudo, B Bader-Meunier, EM Baildam, R Battini, MW Beresford, et al., Gain-of-function mutations in IFIH1 cause a spectrum of human disease phenotypes associated with upregulated type I interferon signaling. Nat Genet. 46(5): p. 503-9.

49. Goubau D, S Deddouche, and C Reis e Sousa, Cytosolic sensing of viruses. Immunity. 38(5): p. 855-69.

50. Morita M, G Stamp, P Robins, A Dulic, I Rosewell, G Hrivnak, G Daly, T Lindahl, and DE Barnes, Gene-targeted mice lacking the Trex1 (DNase Ⅲ) 3'-->5' DNA exonuclease develop inflammatory myocarditis. Mol Cell Biol, 2004. 24(15): p. 6719-27.

51. Stetson DB, JS Ko, T Heidmann, and R Medzhitov, Trex1 prevents cell-intrinsic initiation of autoimmunity. Cell, 2008. 134(4): p. 587-98.

52. Gall A, P Treuting, KB Elkon, YM Loo, M Gale, Jr., GN Barber, and DB Stetson, Autoimmunity initiates in nonhematopoietic cells and progresses via lymphocytes in an interferon-dependent autoimmune disease. Immunity, 2012. 36(1): p. 120-31.

53. Yang YG, T Lindahl, and DE Barnes, Trex1 exonuclease degrades ssDNA to prevent chronic checkpoint activation and autoimmune disease. Cell, 2007. 131(5): p. 873-86.

54. Yan N, AD Regalado-Magdos, B Stiggelbout, MA Lee-Kirsch, and J Lieberman, The cytosolic exonuclease TREX1 inhibits the innate immune response to human immunodeficiency virus type 1. Nat Immunol, 2010. 11(11): p. 1005-13.

55. Hartner JC, CR Walkley, J Lu, and SH Orkin, ADAR1 is essential for the maintenance of hematopoiesis and suppression of interferon signaling. Nat Immunol, 2009. 10(1): p. 109-15.

56. Reijns MA, B Rabe, RE Rigby, P Mill, KR Astell, LA Lettice, S Boyle, A Leitch, M Keighren, F Kilanowski, et al., Enzymatic removal of ribonucleotides from DNA is essential for mammalian genome integrity and development. Cell. 149(5): p. 1008-22.

57. Hiller B, M Achleitner, S Glage, R Naumann, R Behrendt, and A Roers, Mammalian RNase H2 removes ribonucleotides from DNA to maintain genome integrity. J Exp Med. 209(8): p. 1419-26.

58. Rehwinkel J, J Maelfait, A Bridgeman, R Rigby, B Hayward, RA Liberatore, PD Bieniasz, GJ Towers, LF Moita, YJ Crow, et al., SAMHD1-dependent retroviral control and escape in mice. EMBO J. 32(18): p. 2454-62.

59. Behrendt R, T Schumann, A Gerbaulet, LA Nguyen, N Schubert, D Alexopoulou, U Berka, S Lienenklaus, K Peschke, K Gibbert, et al., Mouse SAMHD1 has antiretroviral activity and suppresses a spontaneous cell-intrinsic antiviral response. Cell Rep. 4(4): p. 689-96.

60. Manel N, B Hogstad, Y Wang, DE Levy, D Unutmaz, and DR Littman, A cryptic sensor for HIV-1 activates antiviral innate immunity in dendritic cells. Nature, 2010. 467(7312): p. 214-7.

61. Rohman M and KJ Harrison-Lavoie, Separation of copurifying GroEL from glutathione-S-transferase fusion proteins. Protein Expr Purif, 2000. 20(1): p. 45-7.

62. Niranjanakumari S, E Lasda, R Brazas, and MA Garcia-Blanco, Reversible cross-linking combined with immunoprecipitation to study RNA-protein interactions in vivo. Methods, 2002. 26(2): p. 182-90.

63. Jiang M, J Mak, A Ladha, E Cohen, M Klein, B Rovinski, and L Kleiman, Identification of tRNAs incorporated into wild-type and mutant human immunodeficiency virus type 1. J Virol, 1993. 67(6): p. 3246-53.

64. Welbourn S, SM Dutta, OJ Semmes, and K Strebel, Restriction of virus infection but not catalytic dNTPase activity is regulated by phosphorylation of SAMHD1. J Virol, 2013. 87(21): p. 11516-24.

65. Matos RG, A Barbas, and CM Arraiano, RNase R mutants elucidate the catalysis of structured RNA: RNA-binding domains select the RNAs targeted for degradation. Biochem J, 2009. 423(2): p. 291-301.

66. Barbas A, RG Matos, M Amblar, E Lopez-Vinas, P Gomez-Puertas, and CM Arraiano, New insights into the mechanism of RNA degradation by ribonuclease Ⅱ: identification of the residue responsible for setting the RNase Ⅱ end product. J Biol Chem, 2008. 283(19): p. 13070-6.

67. Arraiano CM, A Barbas, and M Amblar, Characterizing ribonucleases in vitro examples of synergies between biochemical and structural analysis. Methods Enzymol, 2008. 447: p. 131-60.

68. Mizrahi V, MT Usdin, A Harington, and LR Dudding, Site-directed mutagenesis of the conserved Asp-443 and Asp-498 carboxy-terminal residues of HIV-1 reverse transcriptase. Nucleic Acids Res, 1990. 18(18): p. 5359-63.

69. Hofmann H, EC Logue, N Bloch, W Daddacha, SB Polsky, ML Schultz, B Kim, and NR Landau, The Vpx lentiviral accessory protein targets SAMHD1 for degradation in the nucleus. J Virol, 2012. 86(23): p. 12552-60.

70. Brandariz-Nunez A, JC Valle-Casuso, TE White, N Laguette, M Benkirane, J Brojatsch, and F Diaz-Griffero, Role of SAMHD1 nuclear localization in restriction of HIV-1 and SIVmac. Retrovirology, 2012. 9: p. 49.

71. Ayinde D, N Casartelli, and O Schwartz, Restricting HIV the SAMHD1 way: through nucleotide starvation. Nat Rev Microbiol, 2012. 10(10): p. 675-80.

72. Franzolin E, G Pontarin, C Rampazzo, C Miazzi, P Ferraro, E Palumbo, P Reichard, and V Bianchi, The deoxynucleotide triphosphohydrolase SAMHD1 is a major regulator of DNA precursor pools in mammalian cells. Proc Natl Acad Sci U S A, 2013. 110(35): p. 14272-7.

73. Descours B, A Cribier, C Chable-Bessia, D Ayinde, G Rice, Y Crow, A Yatim, O Schwartz, N Laguette, and M Benkirane, SAMHD1 restricts HIV-1 reverse transcription in quiescent CD4(+) T-cells. Retrovirology, 2012. 9: p. 87.

74. Davidson MB, Y Katou, A Keszthelyi, TL Sing, T Xia, J Ou, JA Vaisica, N Thevakumaran, L Marjavaara, CL Myers, et al., Endogenous DNA replication stress results in expansion of dNTP pools and a mutator phenotype. EMBO J, 2012. 31(4): p. 895-907.

75. Ibrahim H, J Wilusz, and CJ Wilusz, RNA recognition by 3'-to-5' exonucleases: the substrate perspective. Biochim Biophys Acta, 2008. 1779(4): p. 256-65.

76. Ross J, mRNA stability in mammalian cells. Microbiol Rev, 1995. 59(3): p. 423-50.

77. Jern P and JM Coffin, Effects of retroviruses on host genome function. Annu Rev Genet, 2008. 42: p. 709-32.

국 문 초 록

AGS는 유전적인 질병으로 환자에게서 핵산매개면역반응에 의한 자가면역질환 증상이 나타난다. AGS와 관련된 돌연변이 유전자 중에는 *SAMHD1*이 있다. SAMHD1은 HIV-1 억제인자로 작용하여 세포분열이 일어나지 않는 대식세포, 수지상 세포, 휴지상태의 $CD4^+$ T 세포에서 HIV-1의 역전사 과정을 방해한다. SAMHD1은 dNTP를 분해하는 효소 활성을 가지고 있으며 dGTP가 다른 자리 조절자로써 dNTPase 효소 활성을 갖도록 한다. 따라서 SAMHD1은 세포내 dNTP의 양을 줄임으로써 HIV-1의 복제를 저해한다고 연구되었다. 그러나 최근 보고에 따르면, SAMHD1의 dNTPase 활성과 관계없이 SAMHD1 단백질 인산화 여부에 따라 HIV-1의 복제를 억제하는 능력이 조절되는데, 이는 SAMHD1의 또 다른 역할이 있음을 시사한다. 본 연구에서는 SAMHD1이 RNA 분해효소 기능을 가지고 있음을 밝혔으며 이 효소 기능이 HIV-1을 억제하는데 필수적임을 보였다. AGS 질병과 관련된 SAMHD1의 돌연변이와 dGTP가 결합하지 못하는 돌연변이 SAMHD1을 이용하여 2가지 효소 작용 중에 어떤 것이 HIV-1 억제에 중요한지에 대해서 확인하였다. RNA 분해효소 활성만 가지고 있는 $SAMHD1_{D137N}$의 경우는 HIV-1를 억제할 수 있었으나 dNTPase 활성만 가지는 $SAMHD1_{Q548A}$는 HIV-1 복제를 막을 수 없었다. 이는 SAMHD1의 RNA 분해효소 활성이 HIV-1

억제 기작의 핵심이라는 것을 의미한다. 실제 SAMHD1은 HIV-1 감염초기에 직접 HIV-1 유전체 RNA에 결합하여 분해함으로써 HIV-1 생활사에 타격을 입히는 것으로 확인되었다. 인간의 대식세포나 $CD4^+$ T 세포에 SAMHD1의 발현을 감소시켰을 때, HIV-1 유전체 RNA가 안정화 되는 실험적 결과를 이를 뒷받침한다. 또한 592번째 아미노산인 트레오닌의 인산화에 의한 HIV-1의 억제 기능 조절은 SAMHD1의 HIV-1 유전체 RNA 분해 작용에 대한 조절로 이루어짐을 보였다. 여러 실험 결과들을 통해 나는 SAMHD1이 가지는 두 가지 효소 활성 중에서 dNTPase가 아닌 RNase 효소 활성이 HIV-1를 억제하는데 중요하다는 것을 밝혔다.

주요어: HIV-1, SAMHD1, RNA 분해효소

학 번: 2008-20250